Zoosyst. Evol. 102 (3) 2026, 783–805 | DOI 10.3897/zse.102.181547

PENSOFT

für Natur MUSEUM FÜR NATURKUNDE BERLIN

Unveiling cryptic diversity: two new species of *Dugesia* from northern China, including one sibling species (Platyhelminthes, Tricladida, Dugesiidae)

Yi-Fan Su[1], Fu-Yu Yu[1], Fan Wu[1], Jing-Yi Wang[1], Ronald Sluys[2], De-Zeng Liu[1], Lei Wang[1], Zi-Mei Dong[1], Guang-Wen Chen[1]

1 *College of Life Science, Henan Normal University, Xinxiang, 453007 Henan, China*

2 *Naturalis Biodiversity Center, Darwinweg 2, 2333 CR, Leiden, Netherlands*

https://zoobank.org/73AA6CFB-182E-4AAB-8F01-EAEE92CFFCCF

Corresponding authors: Lei Wang (wangleixx@163.com); Zi-Mei Dong (dzmhjx@163.com); Guang-Wen Chen (chengw0183@sina.com)

Academic editor: Tom Artois ♦ **Received** 8 December 2025 ♦ **Accepted** 4 May 2026 ♦ **Published** 28 May 2026

Abstract

Two new species of *Dugesia* from the Taihang and Funiu Mountains, including one sibling species, are described by applying an integrative approach, including morphological, karyological, histological, and molecular information. *Dugesia cylindrica* Chen & Dong, **sp. nov.** is characterized by the following features, among others: sac-shaped copulatory bursa located immediately posterior to the pharyngeal pocket; stubby, cylindrical penis papilla with a blunt tip; large and pointed diaphragm; a long connecting duct between the seminal vesicle and diaphragm; slightly ventrally displaced ejaculatory duct with a terminal opening; chromosome complement diploid, with 16 metacentric chromosomes. *Dugesia elongata* Chen & Dong, **sp. nov.** is characterized by the following features, among others: barrel-shaped penis papilla; elongated, dumb-bell shaped seminal vesicle; long connecting duct between the seminal vesicle and low-conical diaphragm; ventrally displaced ejaculatory duct opening at the tip of the penis papilla, albeit at its ventral portion; asymmetrical openings of the oviducts; mixoploid karyotype, with diploid metacentric chromosome complements of $2n = 16$ and triploid metacentric complements of $3n = 24$. In the molecular phylogenetic tree, the two new species belong to two different subclades of the group comprising Eastern Palearctic/Oriental/Australasian species, with the two clades forming sister taxa. The distinct specific status of these two new species is also supported by their genetic distances. The distribution records of the two new species underscore the rich diversity of freshwater planarians in this region, and the discovery of the sibling species highlights the efficacy of integrative taxonomy in delimiting cryptic species.

Key Words

Anatomy, Funiu Mountains, karyology, molecular phylogeny, molecular species delimitation, Taihang Mountains, taxonomy

Introduction

The genus *Dugesia* Girard, 1850 (Platyhelminthes, Tricladida, Dugesiidae) represents one of the more extensively studied groups of free-living freshwater flatworms (Sluys et al. 2018). Studies have shown that *Dugesia* is an ancient genus, having reached its present distribution through a complex history of dispersal and vicariant events following its origin in southern Gondwana (Solà et al. 2022). *Dugesia* species inhabit a wide variety of freshwater streams in Africa, Europe, the Middle East, South Asia, and Australasia (Kawakatsu 1968; Sluys et al. 1998). Currently, approximately 117 species of the genus *Dugesia* have been reported from the major portion of the Old World and Australia. However, it was only recently that taxonomic studies started to unveil its rich biodiversity in China, which forms a potential distribution hotspot for this genus (Solà et al. 2022). In China, seventeen species were described from its Oriental Realm (Chen et al. 2022; Wang et al. 2024, 2025; Wu et al. 2025), whereas for its Palearctic Realm, only one new species was reported (Wang et al. 2022).

The Funiu Mountains are the extension of the Qinling Mountains, which form the watershed between the Huaihe and Han River basins (Li et al. 2020, 2024). As parts of China's Central Orogenic Belt, the Funiu Mountains formed through the collision of the Northern China and Yangtze tectonic blocks. These mountains exhibit unique landforms and abundant water resources, which provide a natural environment for high biodiversity (Dong et al. 2022). The occurrence of a *Polycelis* species has been reported in the Qinling Mountains, viz., *P. asiatica* Selivanova, 1985 (Sun et al. 2024).

The Taihang Mountains in China are located at the eastern margin of the Loess Plateau, which experienced several tectonic upheavals in its geological history, such as the Yanshanian, Himalayan, and Lüliangshian orogenic processes (Zhong et al. 2010; Wu et al. 2020). Furthermore, the Taihang Mountains are located in a temperate monsoon climate with abundant rainfall and harbor abundant animal diversity, including freshwater planarians (Wang et al. 2009; Mo et al. 2019). So far, five freshwater planarian species were described from this region, viz., *Polycelis jinglensis* Liu, 1996, *P. jingyuanica* Liu, 1996, *P. wutaishanica* Liu, 1996, *P. yangchengensis* Dong et al., 2017, and *Dugesia constrictiva* Chen & Dong, 2022 (Liu 1996; Dong et al. 2017; Wang et al. 2022).

Previous research suggests that the species diversity of freshwater planarians within the Palearctic Realm of China may be extremely rich (Wang et al. 2022; Sun et al. 2024). Preliminary analyses suggested that there is a sibling species from the Taihang Mountains, which is highly similar to *D. patula*. Recent studies using molecular-based analyses have resulted in the discovery of new species within the genus *Dugesia* (Sluys et al. 2013; Stocchino et al. 2017; Leria et al. 2020; Dols-Serrate et al. 2024a, 2024b). The increasing use of molecular discovery and validation methods in an integrative taxonomic approach may contribute to the resolution of complicated species delimitation in the genus *Dugesia*, such as Automatic Barcode Gap Discovery (ABGD), Assemble Species by Automatic Partitioning (ASAP), General Mixed Yule-Coalescent model (GMYC), and Poisson tree process (PTP) (Leria et al. 2020; Dols-Serrate et al. 2024a, 2024b). In the present paper, a new species that is a sibling species of *Dugesia patula* Chen & Dong, 2025 is described for the Taihang Mountains, as well as a new species of *Dugesia* for both the Taihang Mountains and Funiu Mountains, by applying four different molecular species delimitation methods, together with morphological and anatomical information.

Materials and methods

Specimen collection and culture

Specimens were collected from under stones in a stream with the help of a paintbrush. At collection, over 70 asexual worms and 20 sexual worms of *D. cylindrica* Chen & Dong, sp. nov. were sampled from a small pool formed by a stream flowing down from the southern Taihang Mountains (35°44'28"N, 114°4'34"E; alt. 350 m a.s.l.). In addition, specimens of *D. cylindrica* were also sampled from 2018 to 2023 from three other localities, viz., Shibanyan village (36°9'59"N, 113°42'51"E; alt. 1050 m a.s.l.), Linzhou City, Henan Province; Huairou village (40°35'37"N, 116°34'48"E; alt. 510 m a.s.l.), Beijing City; and Xiaodianhe village (35°36'53"N, 114°0'1"E; alt. 250 m a.s.l.), Weihui City, Henan Province. With respect to *D. elongata* Chen & Dong, sp. nov., over 70 asexual worms and seven sexual worms were collected from a small pool in the Baiyun National Forest Park in the Funiu Mountains (33°54'43"N, 111°83'49"E; alt. 1100 m a.s.l.). In addition, specimens of *D. elongata* were also sampled from another locality, viz., Shuiyunxuan pub, Yangcheng village (35°21'29"N, 112°11'1"E; alt. 1150 m a.s.l.), Jincheng City, Shanxi Province (Fig. 1). After collection, the worms were transferred to plastic bottles filled with spring water, which were placed in a cooler filled with ice bags during transportation to the laboratory.

The planarians were cultured in autoclaved tap water at 16 °C in an automatic incubator and fed with fresh beef liver once per week. The worms were starved for at least 7 days before being used for histological studies and DNA extraction. Images of their external morphology were obtained using a digital camera attached to a stereo-dissecting microscope.

Phylogenetic analysis

Procedures for DNA extraction, amplification, and sequencing followed those detailed in Wang et al. (2025). Fragments of the cytochrome *c* oxidase subunit I (*COI*), internal transcribed spacer 1 (*ITS-1*), 18S ribosomal gene (*18S rDNA*, type II), and 28S ribosomal gene (*28S rDNA*) were amplified using specific primers (see Suppl. material 2 for sequences and annealing temperatures). For the two new species, three specimens were examined from each of their respective type localities (LMG for *D. cylindrica* and JJM for *D. elongata*). In addition, one specimen was examined from each of the three paratype localities for *Dugesia cylindrica* (LZSXG, BJHR, XDH) and one paratype locality of *Dugesia elongata* (SYXKZ). Specimens were used for DNA extraction, from which *COI*, *ITS-1*, 18S, and 28S were amplified. Phylogenetic analyses were performed based on the two new *Dugesia* species and available sequences of 52 other *Dugesia* species from major portions of the geographic range of the genus, while *Schmidtea mediterranea* (Benazzi et al., 1975), *S. polychroa* (Schmidt, 1861), and *Recurva postrema* Sluys & Solà, 2013 were chosen as the outgroup taxa (Table 1).

Sequences of *ITS-1*, *18S*, and *28S* were aligned online with MAFFT (Online Version 7.247; https://mafft.cbrc.jp/alignment/server/) using the G-INS-i algorithms (Katoh

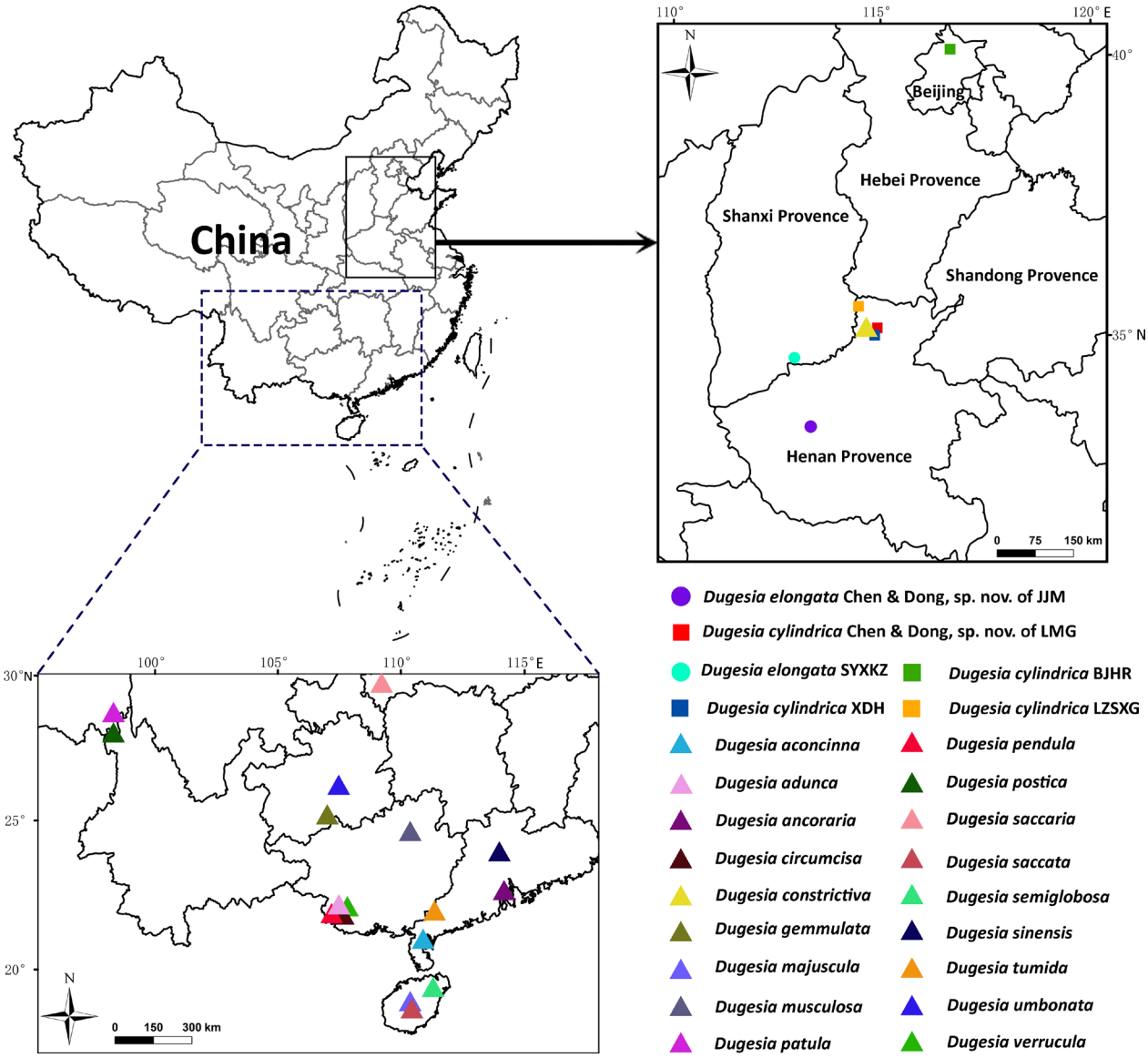

Figure 1. Map showing the distribution of *Dugesia* species across China, including the sampling localities of the new species from the Taihang Mountains and Funiu Mountains.

et al. 2013). Protein-coding *COI* sequences were translated into amino acid sequences to check for the presence of stop codons using NCBI's genetic code 9—Flatworm Mitochondrial. *COI* sequences were aligned with Translator X (Abascal et al. 2010, http://translatorx.co.uk) using the FFT-NS-2 method, checked by BioEdit 7.2.6.1 (Hall et al. 1999), and, thereafter, back-translated to nucleotide sequences. Since automated removal of gap columns and variable regions has been reported to negatively affect the accuracy of the inferred phylogeny (Dessimoz et al. 2010; Tan et al. 2015), the Gblocks option was not applied to the alignments (Talavera and Castresana 2007). A total of four datasets were used in this study, viz., dataset I: *ITS-1* (58 sequences; Table 1), dataset II: *COI* (64 sequences; Table 1), dataset III: concatenated sequences *COI* + *ITS-1* + *28S rDNA* + *18S rDNA* (219 sequences; Table 1), and dataset IV: *COI* (23 known *Dugesia* species from the Eastern Palearctic/Oriental/Australasian clade only and the two new species, 31 sequences; Table 1).

Dataset III for the phylogenetic analysis consisted of a total of 4298 base pairs (bp). The Bayesian information criterion (BIC) was implemented in PartitionFinder 2 (Lanfear et al. 2012, 2017) to estimate the best-fit partition schemes and models of the concatenated sequences. The best models for each gene and codon position were GTR + G for *ITS-1* and GTR + I + G for the three codon positions of *COI*, *18S*, and *28S*. Maximum likelihood (ML) analysis was conducted by IQ-TREE in PhyloSuite v1.2.3pre3 (Zhang et al. 2020) with 10,000 standard bootstrap repetitions, using the best-fit substitution model. Bayesian inference (BI) analysis was conducted with MrBayes v3.2.4 (Ronquist et al. 2012) under the same model as ML analysis. Two replicate runs were used, using four Markov chain Monte Carlo (MCMC) calculations for 5,000,000 generations, sampling every 1000 generations, with generations being added until the runs had reached a stationary state. The convergence of runs was checked by monitoring that the standard deviation of split frequencies

Table 1. GenBank accession numbers of sequences used in molecular analyses.

Species	GenBank			
	COI	***ITS-1***	***28S***	***18S***
D. aconcinna	PV055688	PV055833	PV055834	-
D. adunca	OL505739	OL527659	-	-
D. aethiopica	KY498845	KY498785	KY498806	KY498822
D. afromontana	KY498846	KY498786	KY498807	KY498823
D. ancoraria	OR326966	OR296750	OR225689	OR198141
D. arabica	OL410620	OK587374	OK491342	OK646637
D. arcadia	KC006971	KC007044	OK491318	KF308694
D. ariadnae	KC006972	KC007048	OK491317	OK646636
D. batuensis	OL410626	OK587362	OK491316	OK646630
D. benazzii	FJ646977 + FJ646933	FJ646890	MK712509	OK646628
D. bengalensis	-	FJ646897	-	-
D. bifida	KY498851	KY498791	KY498813	KY498843
D. bijuga	MH119630	-	-	MH113806
D. cylindrica LMG-1*	PZ369199	PZ383201	PZ383219	PZ383214
D. cylindrica LMG-2*	PZ369201	PZ383202	PZ380079	PZ383216
D. cylindrica LMG-3*	PZ369200	PZ383203	PZ383221	PZ383215
D. cylindrica BJHR*	PZ369202	PZ383205	PZ383220	PZ380095
D. cylindrica LZSXG*	PZ369198	PZ383210	PZ380055	PZ383211
D. cylindrica XDH*	PZ380216	PZ383204	PZ374709	PZ374708
D. circumcisa	MZ147041	MZ146782	-	-
D. cretica	KC006976	KC007050	OK491340	KF308697
D. constrictiva	MZ871766	MZ869023	-	-
D. damoae	KF308768	KC007057	OK491310	OK646619
D. deharvengi	KF907820	KF907817	KF907824	-
D. effusa	KF308780	KC007058	OK491311	OK646618
D. elegans	KC006984	KC007063	OK491313	KF308695
D. etrusca	FJ646984 + FJ646939	FJ646898	OK491312	OK646617
D. gemmulata	OL632201	-	-	-
D. gibberosa	KY498857	KY498803	KY498819	KY498842
D. gonocephala	FJ646986 + FJ646941	FJ646901	DQ665965	DQ666002
D. granosa	OL410634	KY498795	KY498816	KY498833
D. hepta	MK712639	MK713035	OK491309	OK646612
D. hoidi	OR650791	-	-	-
D. improvisa	KC006987	KC007065	OK491304	KF308696
D. japonica	FJ646990	FJ646904	DQ665966	D83382
D. liguriensis	OL410632	OK587358	OK491353	OK646615
D. malickyi	KC006988	KC007068	OK491294	OK646585
D. majuscula	MW533425	MW533591	-	-
D. mariae	OR650829	-	-	-
D. musculosa	OR189184	OR205922	-	-
D. naiadis	KF308756	OK587343	OK491293	-
D. notogaea	FJ646993 + FJ646945	FJ646908	KJ599720	KJ599713
D. parasagitta	KF308739	KC007073	-	OK646577
D. patula	PV786826	PV788696	PV788698	PV788697
D. pendula	OR195337	OR205921	-	-
D. postica	PV786825	PV788693	PV788694	PV788695
D. pustulata	MH119631	OK587366	OK491355	MH113807
D. ryukyuensis	AB618488	FJ646910	OK491323	AF050433
D. saccata	PV055687	PV055830	PV055832	PV055831
D. sagitta	KC007006	KC007077	OK491320	OK646567
D. elongata JJM-1*	PZ374187	PZ383206	PZ374186	PZ383208

Species	GenBank			
	COI	*ITS-1*	*28S*	*18S*
D. elongata JJM-2*	PZ374680	PZ383207	PZ387733	PZ383213
D. elongata JJM-3*	PZ374681	PZ383209	PZ380311	PZ383218
D. elongata SYXKZ*	PZ374682	PZ383212	PZ374233	PZ383217
D. semiglobosa	MW525210	MW526992	-	-
D. sicula	KF308797	OK587339	OK491287	KF308693
D. sigmoides	KY498849	KY498789	KY498811	KY498827
D. sinensis	KP401592	-	-	-
D. subtentaculata	MK712628	MK713004	MK712501	AF013155
D. tumida	OL505740	OL527709	-	
D. umbonata	MT176641	MT177211	MT177210	MT177214
D. verrucula	MZ147040	MZ146760	-	-
R. postrema	KF308763	-	MG457274	KF308691
S. mediterranea	JF837062	AF047854	DQ665992	U31085
S. polychroa	FJ646975 + FJ647021	-	DQ665993	AF013152

* The new species of this study.

reached a value below 0.01, thus indicating that the runs had reached stationarity. The output parameter files of each run were checked in TRACER v1.7.1 to ensure that the effective sample size (ESS) values for each parameter were greater than 200 (Rambaut et al. 2018). Following completion of each analysis, the first 25% of samples were discarded as "burn-in," and the remaining samples were used to generate a 50% majority rule consensus tree. FigTree v1.4.3 was used to view the tree obtained.

Genetic distances and molecular species delimitation

The genetic distances were calculated by MEGA 6.06 (Tamura et al. 2013; Wang et al. 2024) with the Kimura 2-parameter substitution model (Lázaro et al. 2009; Solà et al. 2013) based on dataset I and dataset II.

For DNA sequence-based species delimitation, dataset IV was analyzed with the following methods: Assemble Species by Automatic Barcode Gap Discovery (ABGD), Automatic Partitioning (ASAP), Poisson tree process (PTP), and the Bayesian implementation of the Poisson Tree Processes (bPTP) model (Puillandre et al. 2011; Zhang et al. 2013; Puillandre et al. 2021).

According to Puillandre et al. (2011), ABGD analysis identifies different sequences into potential species based on limits of divergence. This analysis was performed on the web version of ABGD (https://bioinfo.mnhn.fr/abi/public/abgd/abgdweb.html) based on dataset IV, using a gap width of 1.0. The prior for the maximum value of intraspecific divergence (*P*) was set to range from 0.001 to 0.1, with the number of recursive steps set to default (10).

ASAP (Puillandre et al. 2021) was executed using the ASAP online server (https://bioinfo.mnhn.fr/abi/public/asap) under the Jukes-Cantor model, based on dataset IV. The result of ASAP with the lowest score was considered the optimal group number in the present study.

The bPTP method takes as input a binary, rooted phylogenetic tree inferred with an ML or a BI approach. In this case, the BI analysis of dataset IV was used as the input file on the PTP web server (https://species.h-its.org/ptp/) for delimitation of each operational taxonomic unit (OTU) from each population; the analysis included default parameters. Four independent runs, starting from random trees, were performed with a MCMC chain length of 10 million, sampled every 100,000 generations; the analysis included default parameters.

Histology and karyology

Histological sections were prepared as described previously by Dong et al. (2017). For preparation of histological sections, the worms were fixed in Bouin's fluid for 24 h and subsequently rinsed and stored in 70% ethanol. For histological study, specimens were dehydrated in an ascending series of ethanol solutions, after which they were cleared in clove oil and embedded in synthetic wax. Serial sections were made at intervals of 6 μm and stained with hematoxylin–eosin or with hematoxylin and Cason's Mallory-Heidenhain stain (Winsor and Sluys 2018). Histological preparations of specimens have been deposited in the Zoological Museum of the College of Life Science of Henan Normal University, Xinxiang, China (ZMHNU), and Naturalis Biodiversity Center, Leiden, The Netherlands (RMNH).

The air-drying method was used to obtain karyological preparations, according to the protocols described by Dong et al. (2017) and Wang et al. (2024). In brief, the worms were first cut transversally into three pieces, which were cultured in distilled water for 3 days. Then, the blastemas were treated with a 0.02% colchicine solution at 14 °C for 3 h. Hereafter, blastemas were placed in 0.1% KCl hypotonic solution for 3 h. Subsequently, the blastemas were evenly hammered with an oversized

needle to create a cell suspension and were fixed on a slide for approximately 30 s in each fixative fluid. Subsequently, the dispersed cells were dried at room temperature for 24 h and stained with a 0.5% Giemsa solution for 12–15 min.

Mitotic metaphase chromosomes were observed and photographed under a compound microscope (ZEISS, Axio Scope. A1) equipped with a CoolCube digital camera (MetaSystems, Altlussheim, Germany). Karyograms were prepared using the IKAROS Karyotyping system (MetaSystems, Altlussheim, Germany, https://metasystems-international.com/en/products/ikaros/). Well-spread sets of metaphase plates from randomly selected individuals were used to determine ploidy level, centromeric indices, and relative lengths of the chromosomes. Based on IKAROS artificial intelligence (AI) for karyotyping, the curved or overlapping chromosomes were accurately measured, and their centromeric position was calculated. Hereafter, relative lengths of the chromosomes and centromeric positions were rechecked by manual calibration. In the calculations of the averages, the very few heteromorphic chromosomes and karyotypes that were obtained were not included in the analysis to avoid misleading results and incorrect conclusions. Karyotype parameter measurements were executed as published previously by Chen et al. (2008). Chromosomal nomenclature follows Levan et al. (1964).

Abbreviations used in the figures

bc: bursal canal; ca: common atrium; cb: copulatory bursa; cg: cement glands; coa: copulatory apparatus; d: diaphragm; e: eye; ed: ejaculatory duct; epg: erythrophil penis glands; go: gonopore; lod: left oviduct; lvd: left vas deferens; mo: mouth; ma: male atrium; od: oviduct; ph: pharynx; pp: penis papilla; rod: right oviduct; rvd: right vas deferens; sg: shell glands; spv: spermiducal vesicle; sv: seminal vesicle; vd: vas deferens.

Availability of data and materials

Holotypes and paratypes of the two new species were deposited in the Zoological Museum of the College of Life Science of Henan Normal University, Xinxiang, China (ZMHNU), and Naturalis Biodiversity Center, Leiden, The Netherlands (RMNH).

Results

Molecular phylogeny

Phylogenetic trees were constructed using dataset III, including 705 bp for *COI*, 645 bp for *ITS-1*, 1384 bp for *28S*, and 1564 bp for *18S*. Three specimens were examined from each of the two new species, *Dugesia cylindrica* (LMG) and *D. elongata* (JJM), and these showed no variation in any of *COI*, *ITS-1*, *18S*, and *28S*.

The topologies of the trees generated from the BI and ML analyses were basically congruent, differing only in support values (Fig. 2, Suppl. material 1: fig. S1). In the phylogenetic trees, the species from China all fall into a group comprising Eastern Palearctic/Oriental/Australasian species. This clade consists of two main branches (pp = 0.99, bs = 85). *Dugesia cylindrica* and *D. elongata* belong to two different subclades, which form sister taxa (pp = 0.82, bs = 71). *Dugesia cylindrica* shares a sister-group relationship (pp = 1.00, bs = 100) with a small clade comprising *D. patula* Chen & Dong, 2025 and *D. postica* Chen & Dong, 2025 (pp = 0.88, bs = 73). *Dugesia elongata* is sister to *D. constrictiva* Chen & Dong, 2022 (pp = 1.00, bs = 96), and together they are sister to *D. verrucula* Chen & Dong, 2021 (pp = 1.00, bs = 100). The clade of these three species forms the sister taxon of a clade comprising *D. majuscula* Chen & Dong, 2021, *D. pendula* Chen & Dong, 2024, *D. tumida* Chen & Sluys, 2022, and *D. saccaria* Wang & Sluys, 2024 (pp = 1.00, bs = 100).

Genetic distances

The highest *COI* distance values between *D. cylindrica* and *D. elongata* and their congeners were 23.68–24.49% (*D. cylindrica* with *D. naiadis* Sluys, 2013) and 26.25% (*D. elongata* with *D. bifida* Stocchino & Sluys, 2014), respectively. The lowest *COI* distance values were 4.93–5.56% (*D. cylindrica* with *D. patula*) and 12.02% (*D. elongata* with *D. constrictiva*), respectively. Furthermore, there is a 17.40–17.93% *COI* difference between the two new species (Suppl. material 3). With respect to *ITS-1*, the highest distance values between *D. cylindrica* and *D. elongata* and their congeners were 22.43–22.70% and 20.63% (both with *D. pustulata* Harrath & Sluys, 2019), respectively, while the lowest *ITS-1* distance values were 1.29–1.47% (*D. cylindrica* with *D. patula*) and 1.66% (*D. elongata* with *D. verrucula*), respectively. Furthermore, there is a 7.75% *ITS-1* difference between the two new species (Suppl. material 4).

Molecular species delimitation

The ABGD analysis, performed on dataset IV excluding the outgroup, partitioned the sequences into 22 operational taxonomic units (OTUs). This initial partition was obtained using the Jukes-Cantor (JC69) model, with a prior maximal distance (Pmax) of 0.0551, a barcode gap distance of 0.014, and a Jukes-Cantor MinSlope value of 1.00. It should be noted that the sequence of *D. deharvengi* was removed because it has no common site with the sequence of *D. japonica* Ichikawa & Kawakatsu, 1964, so that the distance

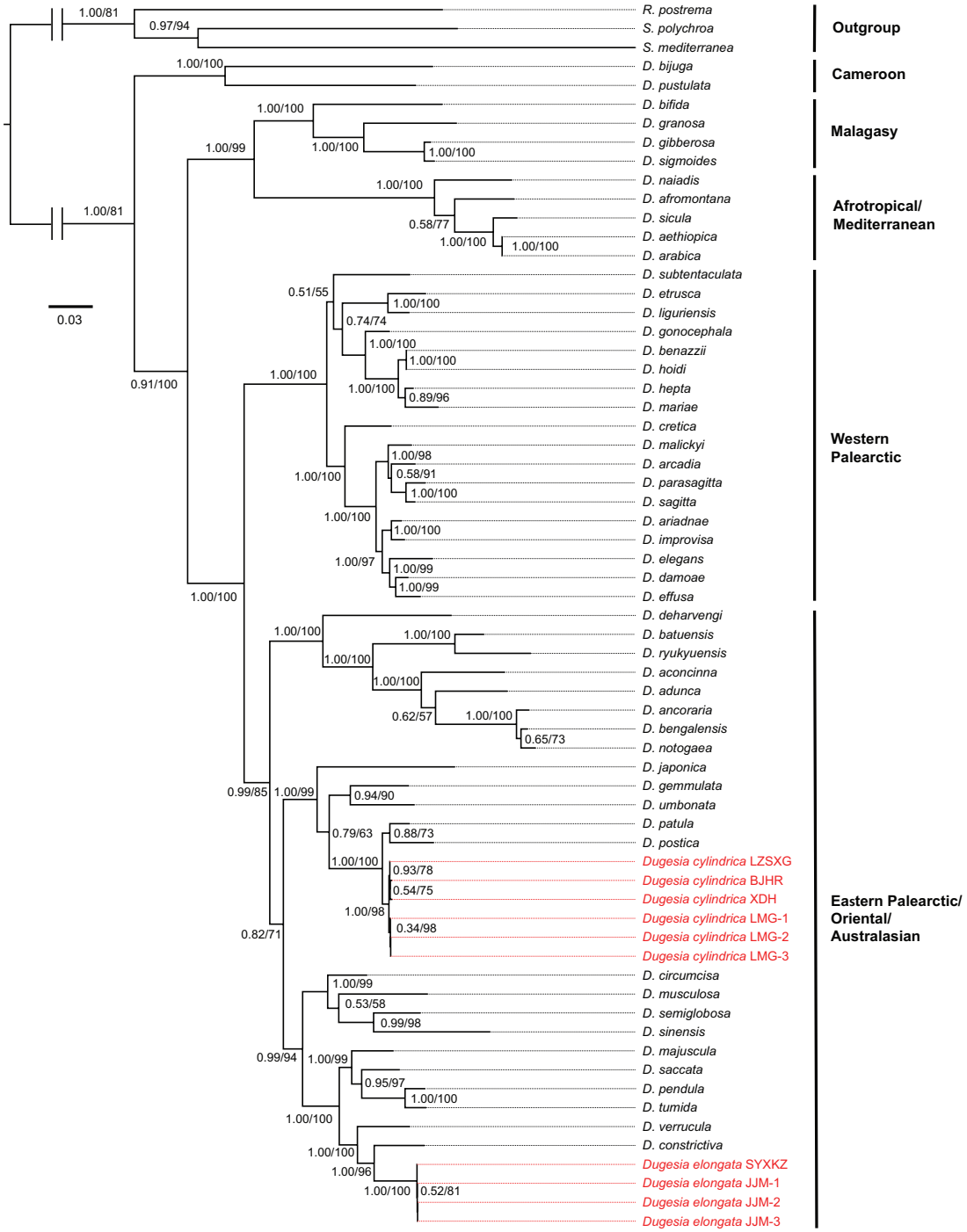

Figure 2. Molecular phylogenetic tree obtained from Bayesian inference of dataset III. Numbers at nodes indicate support values (posterior probability/bootstrap). New species are indicated in red. Scale bar: substitutions per site.

could not be computed. The ASAP analysis identified 10 partitions, ranking them based on the lowest ASAP score. The optimal partition divided the dataset into 22 OTUs, achieving a score of 2.5. The second-best partition identified 20 OTUs with a score of 2.5. Considering that the 22 OTU partition showed complete congruence with the ABGD results (also 22 OTUs) and better reflected the phylogenetic relationships and morphological distinctions observed in the integrative dataset, the 22 OTU partition was adopted as the optimal hypothesis for species delimitation. Importantly, both candidate partitions consistently recognized the populations of *D. cylindrica* and *D. elongata* as distinct OTUs, confirming the status of these two new species regardless of which partition is preferred.

The PTP analysis identified 23 OTUs using the Bayesian approach, generating two output trees based on maximum likelihood (23 OTUs). Compared to ABGD and ASAP, the PTP method resulted in a slightly higher number of splits.

All analyses by these methods revealed that the populations of JJM and SYXKZ were delimited as a single OTU, and the populations of LMG, LZSXG, BJHR, and XDQ were also delimited as a single OTU (Fig. 3).

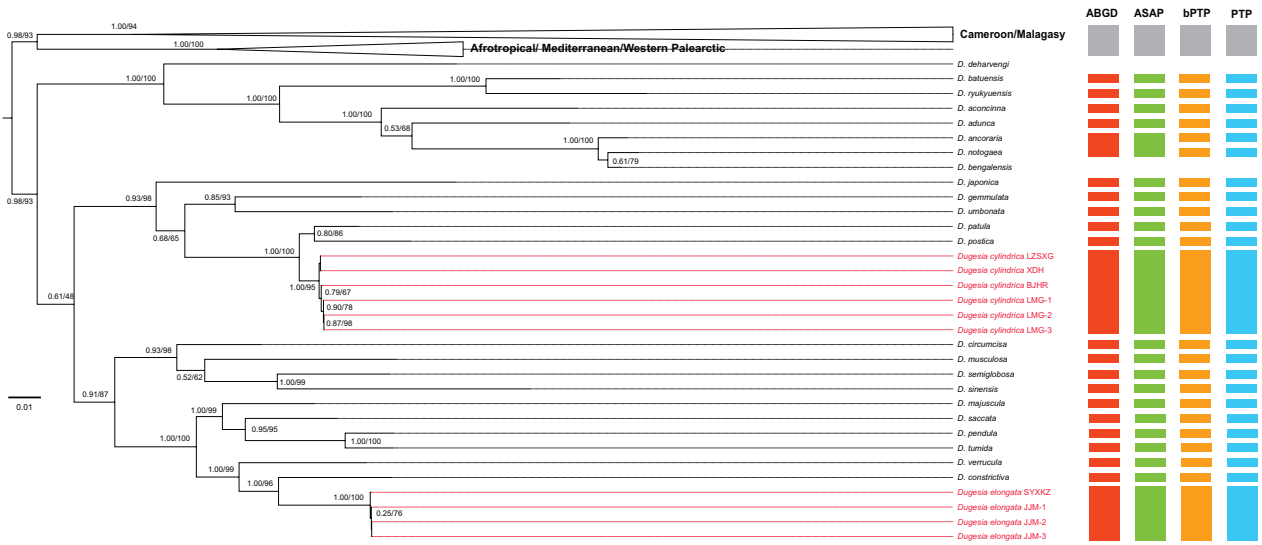

Figure 3. Species discovery delimitation schemes for ABGD, ASAP, PTP, and bPTP based on dataset IV. Numbers at nodes indicate support values (pp/bs). New species are indicated in red. Scale bar: substitutions per site.

Systematic account

Order Tricladida Lang, 1884
Suborder Continenticola Carranza, Littlewood, Clough, Ruiz-Trillo, Baguñà & Riutort, 1998
Family Dugesiidae Ball, 1974
Genus *Dugesia* Girard, 1850

***Dugesia cylindrica* Chen & Dong, sp. nov.**

https://zoobank.org/423A548D-DFB4-4AC7-BA5B-7AFE3A59C4E1

Figs 1, 4–8

Collection site and habitat. On 4 December 2021, the specimens were collected from a small pool formed by a stream flowing down from the southern Taihang Mountains at an altitude of 346 m above sea level (a.s.l.). At the time of collection, the air temperature was 16 °C and the water temperature was 13.7 °C (Figs 1, 4A, B). The water was clear and flowed slowly, and it was used as drinking water by local residents.

Material examined. ***Holotype*:** •ZMHNU—LMG3, Laomugou village (35°44'28"N, 114°4'34"E; alt. 350 m a.s.l.), Hebi City, Henan Province, China, 4 December 2021, coll. G-W Chen, Z-M Dong and co-workers, sagittal sections on 36 slides.

***Paratypes*:** •ZMHNU—LMG4-6, ibid., sagittal sections on 41, 37, 40 slides, respectively; •RMNH.VER.22726.1, ibid., sagittal sections on 46 slides; •RMNH.VER. 22726.2, ibid., sagittal sections on 45 slides; •ZMHNU—LMG8, ibid., horizontal sections on 13 slides; •ZMHNU—LMG 7, 9, and 10, ibid., transverse sections on 24, 32 and 36 slides, respectively.

***Other material*:** •ZMHNU—LZSXG1, 5, 6, Shibanyan village (36°9'59"N, 113°42'51"E; alt. 1050 m a.s.l.), Linzhou City, Henan Province, sagittal sections on 12, 69, and 57 slides, respectively; •ZMHNU—LZSXG2, 7, ibid., horizontal sections on 25 and 9 slides; •ZMHNU—LZSXG4, 8, ibid., transverse sections on 29 and 28 slides, respectively. •RMNH.VER.22727.1, ibid., sagittal sections on 32 slides.

•ZMHNU—BJHR2-4, Huairou village (40°35'37"N, 116°34'48"E; alt. 510 m a.s.l.), Beijing City, sagittal sections on 37, 59, and 18 slides, respectively. •RMNH.VER.22728.1, ibid., sagittal sections on 56 slides.

•ZMHNU—XDH1, 2, 5, Xiaodianhe village (35°36'53"N, 114°0'1"E; alt. 250 m a.s.l.), Weihui City, Henan Province, sagittal sections on 13, 19, and 21 slides, respectively; •ZMHNU—XDH4, ibid., horizontal sections on 21 slides; •ZMHNU—XDH3, ibid., transverse sections on 27 slides, respectively. •RMNH.VER.22729.1, ibid., sagittal sections on 24 slides.

Diagnosis. *Dugesia cylindrica* is characterized by the presence of the following features: a sac-shaped copulatory bursa that is located immediately posterior to the pharyngeal pocket; stubby, cylindrical penis papilla with a blunt tip; symmetrical openings of the oviducts into the bursal canal at the point where it communicates with the common atrium; vasa deferentia separately and symmetrically opening into the mid-lateral portion of the seminal vesicle; relatively large and pointed diaphragm; a long connecting duct between seminal vesicle and diaphragm; slightly ventrally displaced ejaculatory duct with a terminal opening. Anatomically, *D. cylindrica* is very similar to *D. patula*, but in the latter the copulatory bursa is located at some distance behind the pharyngeal pocket, whereas in the former the bursa lies immediately posterior to the pharyngeal pouch.

Etymology. The specific epithet is derived from the Latin *cylindrus*, cylindrical, and alludes to the blunt and cylindrical penis papilla.

Karyology. Eight intact specimens were randomly selected to prepare metaphase plates. In total, 168 metaphase plates were examined, in which 160 plates exhibited diploid chromosome complements of $2n = 2x = 16$, while the remaining eight plates could not be determined

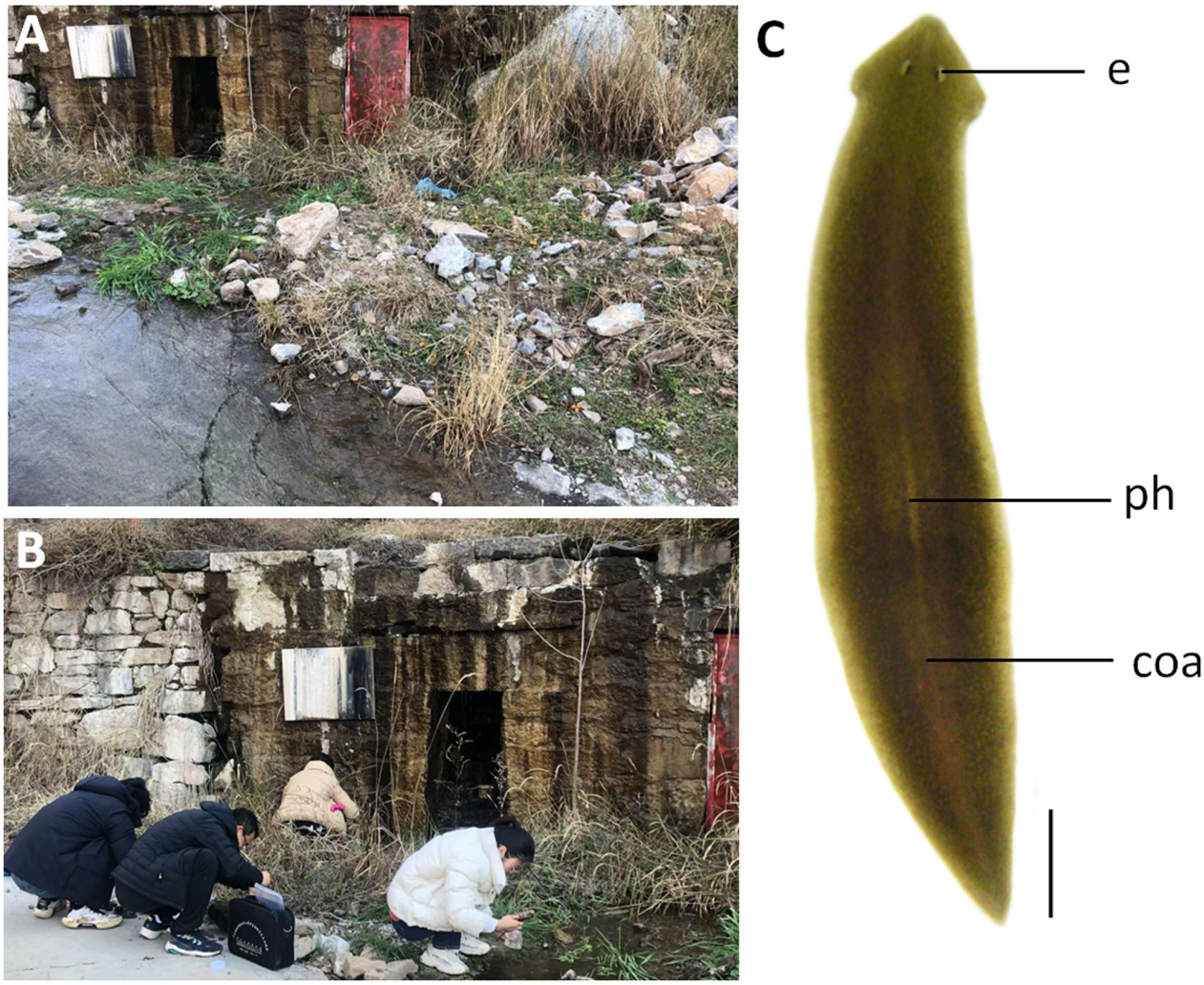

Figure 4. Habitat and external appearance of *Dugesia cylindrica*. **A, B.** Sampling site and habitat; **C.** Sexually mature, live individual. Scale bar: 2 mm. Abbreviations: coa, copulatory apparatus; e, eye; ph, pharynx.

due to either a lack of well-dispersed chromosomes or over-dispersed sets of chromosomes. All eight specimens exhibited diploid chromosome complements, and all chromosomes were metacentric. Karyotype parameters, including relative length, arm ratio, and centromeric index, are given in Table 2. Chromosomal plates and the idiogram are shown in Fig. 5.

Description. Living asexual specimens measured 10–14 mm in length and 1.2–2.1 mm in width, while sexual specimens were 15–19 mm in length and 1.5–2.2 mm in width. The low-triangular head is provided with two blunt auricles and with two eyes, which are located in pigment-free patches. Each pigmented eyecup houses numerous light-sensitive cells. The dorsal surface of the body is dark brown, with a pale, broad margin. The ventral surface is lighter in color than the dorsal one (Fig. 4C).

The pharynx is located at ca. 2/5 of the body length (as determined from the anterior margin), measuring approximately 1/6 of the body length (Fig. 4C). The mouth opening is located at the posterior end of the pharyngeal pocket. Outer pharyngeal musculature is composed of a subepithelial

Table 2. Karyotype parameters (mean values and standard deviations) of *Dugesia cylindrica* Chen & Dong, sp. nov.; m, metacentric.

Chromosome	Relative length	Arm ratio	Centromeric index	Chromosome type
1	18.30 ± 0.64	1.24 ± 0.08	44.77 ± 1.74	m
2	15.59 ± 0.52	1.11 ± 0.13	48.38 ± 1.02	m
3	13.33 ± 0.13	1.24 ± 0.13	44.96 ± 2.32	m
4	12.47 ± 0.25	1.22 ± 0.21	45.34 ± 1.99	m
5	11.45 ± 0.16	1.27 ± 0.05	44.14 ± 0.99	m
6	10.40 ± 0.17	1.19 ± 0.10	45.77 ± 1.97	m
7	9.73 ± 0.39	1.19 ± 0.12	45.82 ± 2.44	m
8	8.72 ± 0.35	1.25 ± 0.14	44.78 ± 2.59	m

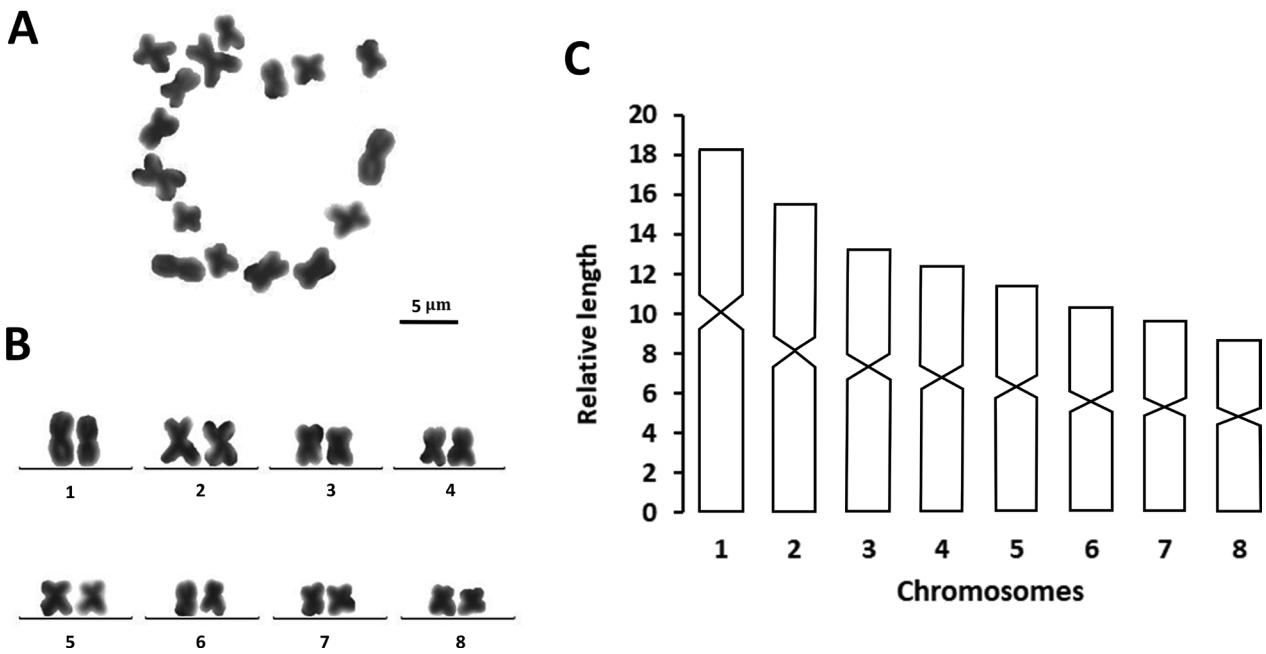

Figure 5. *Dugesia cylindrica*. **A.** Metaphase plate of diploid complement; **B.** Karyogram of diploid complement; **C.** Idiogram. Scale bar: 5 µm.

layer of longitudinal muscles, followed by a thin layer of circular muscles; an extra inner layer of longitudinal muscles was not observed. The inner pharyngeal musculature consists of a subepithelial and thick layer of circular muscle, followed by a thin layer of longitudinal muscle.

In all specimens in which the ovaries could be examined (except LMG-6), the gonads were not hyperplasic, occupying 1/3 of the dorsoventral space. The ovaries are located at a considerable distance behind the brain, i.e., at approximately 1/4th of the distance between the brain and the root of the pharynx. The oviducts extend from the postero-dorsal wall of the ovaries towards the level of the genital pore along the ventral side of the body, where they curve towards the dorsal body surface to open symmetrically into the bursal canal at the point where the canal communicates with the common atrium. The oviducts are lined with a columnar, infranucleated epithelium. Cyanophil shell glands discharge their secretion into the vaginal region of the bursal canal around the oviducal openings. (Fig. 6A, E).

A large, sac-shaped copulatory bursa is situated immediately posterior of the pharyngeal pocket and occupies most of the dorso-ventral space. The bursa is lined by a stratified, columnar, vacuolated, and nucleated epithelium; it is devoid of any surrounding musculature; some bursae contain large clumps of sperm, located within a spermatophore (LMG-1 and 4). The bursal canal runs from the mid-posterior wall of the bursa in caudal direction, slightly to the left side of the male copulatory apparatus. The canal has a width of approximately 1/7 to 1/5 of the dorso-ventral space. At the level of the gonopore, the bursal canal curves ventrally to open into the common atrium. The bursal canal is lined with a ciliated epithelium with basal nuclei and shows a smooth inner wall and has a uniform diameter. The bursal canal is surrounded by three layers of muscle, a subepithelial, thin layer of longitudinal muscles, followed by a thick layer of circular muscle, which is bounded by a thin layer of longitudinal muscles, forming the ectal reinforcement layer. This ectal reinforcement musculature extends from the atrium to 3/4 of the bursal canal.

The small and rounded testes are located on the dorsal side, occupying 1/3 of the dorso-ventral space. Testicular follicles extend from the posterior level of the ovaries to the posterior end of the body. Mature spermatozoa are present in the testes.

The vasa deferentia expand to form spermiducal vesicles at the level of the pharynx and are filled with mature spermatozoa. At the level of the penis bulb, the spermiducal vesicles curve dorso-medially, decrease considerably in diameter, forming narrow ducts, and subsequently penetrate the penis bulb to open symmetrically into the mid-lateral section of the seminal vesicle (Fig. 6D). The sperm ducts are lined with a nucleated epithelium and surrounded by a layer of circular muscle.

The sac-shaped seminal vesicle occupies a major portion of the penis bulb (Fig. 6A, C) and is lined by a flat, nucleated epithelium. The vesicle is surrounded by a well-developed coat of irregularly, crosswise arranged muscle fibers. A well-developed and long duct extends from the posterior wall of seminal vesicle and opens into the ejaculatory duct via a diaphragm. This connecting duct is lined with an infranucleated epithelium, which is underlain by a subepithelial layer of intermingled muscle fibers. The diaphragm is located at approximately 2/3 of the length of the penis papilla and receives the openings of erythrophil penis glands (Fig. 6A). The relatively large and pointed diaphragm opens into a very broad as well as short ejaculatory duct, which is lined with a cuboidal, infranucleated epithelium and is devoid of any discernible musculature. The short ejaculatory duct has

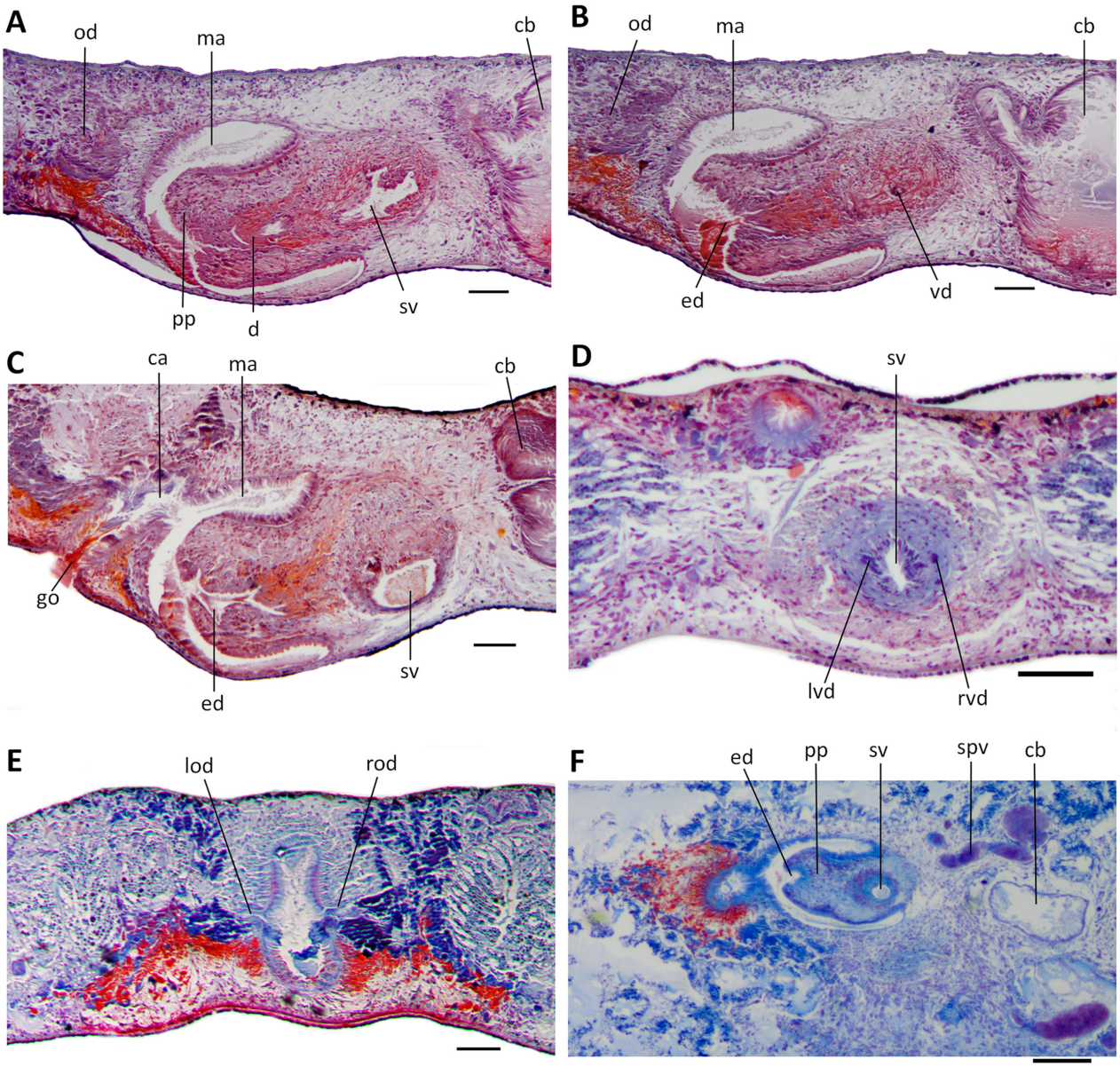

Figure 6. *Dugesia cylindrica*. Photomicrographs. **A.** Sagittal section of holotype LMG3, showing penis papilla, seminal vesicle, diaphragm, male atrium, oviduct, and copulatory bursa; **B.** Sagittal section of holotype LMG3, showing penis papilla, openings of ejaculatory duct, male atrium, oviduct, and copulatory bursa; **C.** Sagittal section of paratype LMG6, showing penis papilla, seminal vesicle, ejaculatory duct, common atrium, male atrium, and gonopore; **D.** Transverse section of paratype LMG7, showing seminal vesicle and symmetric openings of vasa deferentia; **E.** Transverse section of paratype LMG10, showing symmetric openings of the two oviducts; **F.** Horizontal section of paratype LMG8, showing penis papilla, seminal vesicle, and ejaculatory duct. Scale bars: 100 µm.

an extremely broad opening at the blunt tip of the penis papilla. In several specimens, a spermatophore protruded from the opening of the ejaculatory duct at the tip of the penis papilla. With respect to the stubby, cylindrical penis papilla, the slightly ventrally displaced ejaculatory duct causes a slight asymmetry, with the dorsal lip being only marginally larger than the ventral lip. The penis papilla is covered with a nucleated epithelium, which is underlain by a subepithelial layer of circular muscle, followed by a layer of longitudinal muscle fibers (Fig. 6A–C).

The genital atrium is divided into the common atrium and the male atrium, connected through a canal. The common atrium communicates with a gonoduct and leads to the gonopore, which is lined by a columnar epithelium and receives the openings of erythrophil cement glands (Fig. 6A–C).

Reproduction. The worms were collected at 16 °C, and approximately one-third of all the worms were sexually mature in the field. After 3 months of laboratory culturing (at 16 °C), the asexual specimens continuously sexualized and then produced infertile cocoons, as no juveniles hatched from these cocoons. Asexual reproductive behavior with broken tail regeneration was observed in asexual specimens.

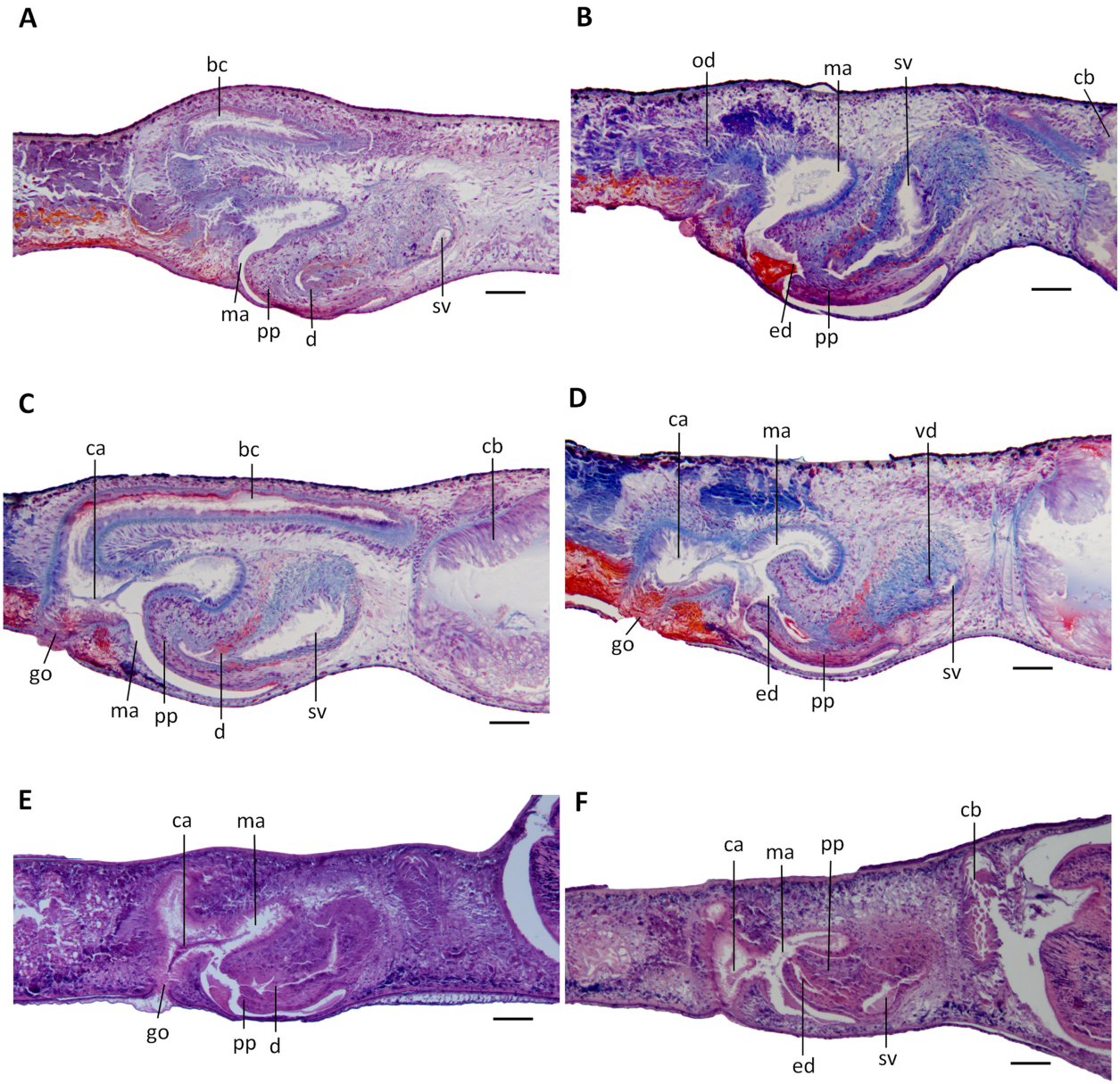

Figure 7. *Dugesia cylindrica*. Photomicrographs of sagittal sections. **A.** Specimen LZSXG3, showing penis papilla, seminal vesicle, diaphragm, male atrium, and bursal canal; **B.** Specimen LZSXG5, showing penis papilla, seminal vesicle, openings of ejaculatory duct, male atrium, oviduct, and copulatory bursa; **C.** Specimen RMNH.VER.22728.1, showing penis papilla, seminal vesicle, diaphragm, copulatory bursa, bursal canal, male atrium, common atrium, and gonopore; **D.** Specimen BJHR3, showing penis papilla, seminal vesicle, vas deferens, openings of ejaculatory duct, male atrium, common atrium, and gonopore; **E.** Specimen XDH1, showing penis papilla, diaphragm, male atrium, common atrium, and gonopore; **F.** Specimen RMNH.VER.22729.1, showing penis papilla, seminal vesicle, openings of ejaculatory duct, male atrium, common atrium, and copulatory bursa. Scale bars: 100 μm.

Discussion. Evidently, *D. cylindrica* is anatomically very similar to *D. patula*. However, the copulatory bursa of *D. patula* is located at a considerable distance (approximately 400–600 μm) behind the pharyngeal pocket, while its length is approximately twice the dorsoventral diameter of the body, i.e., measuring approximately 600–800 μm. This contrasts with the sac-shaped copulatory bursa located immediately posterior to the pharynx in *D. cylindrica*. In view of the fact that the position of the bursa appears to be different in *D. patula* and the molecular information suggests that it is different from *D. cylindrica*, the two species should be considered sibling species.

In addition, *Dugesia cylindrica* exhibits a combination of features that sets it immediately apart from other congeners, in particular, the presence of a ventrally displaced short ejaculatory duct with a terminal opening, as well as a duct between the seminal vesicle and diaphragm. The specimens from the three other localities are consistent with those from the type site (Fig. 7). Many species of *Dugesia* show similar anatomical features. However, there are only three Chinese species with a diaphragm located near the tip of the penis papilla, viz., *D. tumida*, *D. postica*, and *D. patula* (Chen et al. 2022; Wu et al. 2025). However, *D. cylindrica* cannot be synonymized with any of these species. *Dugesia tumida*

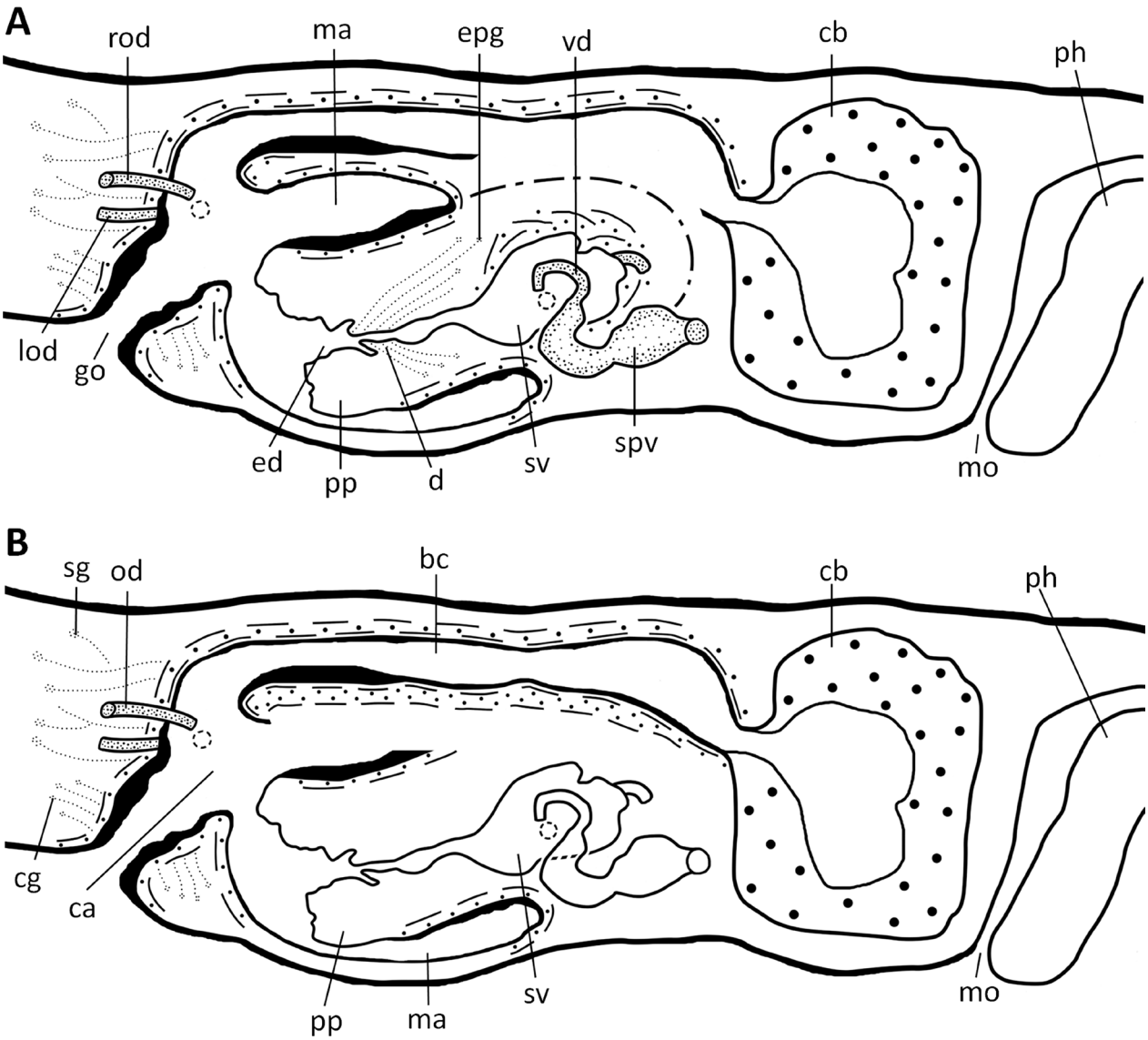

Figure 8. *Dugesia cylindrica*. Sagittal reconstruction of the copulatory apparatus of holotype LMG3. **A.** Sagittal reconstruction of female copulatory apparatus; **B.** Sagittal reconstruction of male copulatory apparatus. Scale bar: 100 µm.

possesses a large, symmetrical penial valve from the middle of which arises the small, distal section of the penis papilla; such a valve is absent in *D. cylindrica*. *Dugesia postica* possesses a large and long penis papilla with a small, dorsal bulge; such a bulge is absent in *D. cylindrica*. In addition, the small diaphragm of *D. postica* is different from the relatively large and pointed diaphragm of *D. cylindrica*.

The karyotype of *D. cylindrica* exhibits a diploid set ($2n = 2x = 16$), with a basic chromosome number of 8. In *Dugesia* species from China, chromosome portraits similar to that of *D. cylindrica* have been documented for *D. constrictiva* and *D. musculosa*. Evidently, the two species are anatomically dissimilar to *D. cylindrica*. *Dugesia constrictiva* has a laterally compressed seminal vesicle, and *D. musculosa* has a bursal canal provided with a strong, thick layer of circular muscle, which extends from the copulatory bursa to the common atrium and gonoduct, which is absent in *D. cylindrica*. However, the karyotype of *D. musculosa* exhibits a complex diploid set ($2n = 2x = 16$ and 16-7th-8th), while aneuploidy is not observed in *D. cylindrica*.

Although *D. cylindrica*, *D. patula*, and *D. postica* belong to a relatively small clade in the phylogenetic tree (Fig. 2) and *D. cylindrica* has the lowest genetic distance with *D. patula*, notably, each species occupies its own branch, while they are anatomically different, albeit only marginally in the case of *D. cylindrica* and *D. patula*. The separate species status of *D. cylindrica* is also supported by the molecular species delimitation results.

Dugesia elongata Chen & Dong, sp. nov.

https://zoobank.org/17E87280-7533-45DC-9636-CE4DAC91703C

Figs 1, 9–12

Collection site and habitat. On 25 October 2021, the specimens were collected from a small pool formed by a stream flowing down from Baiyun Mountain at an altitude of 1100 m a.s.l., an air temperature of 8 °C, and a

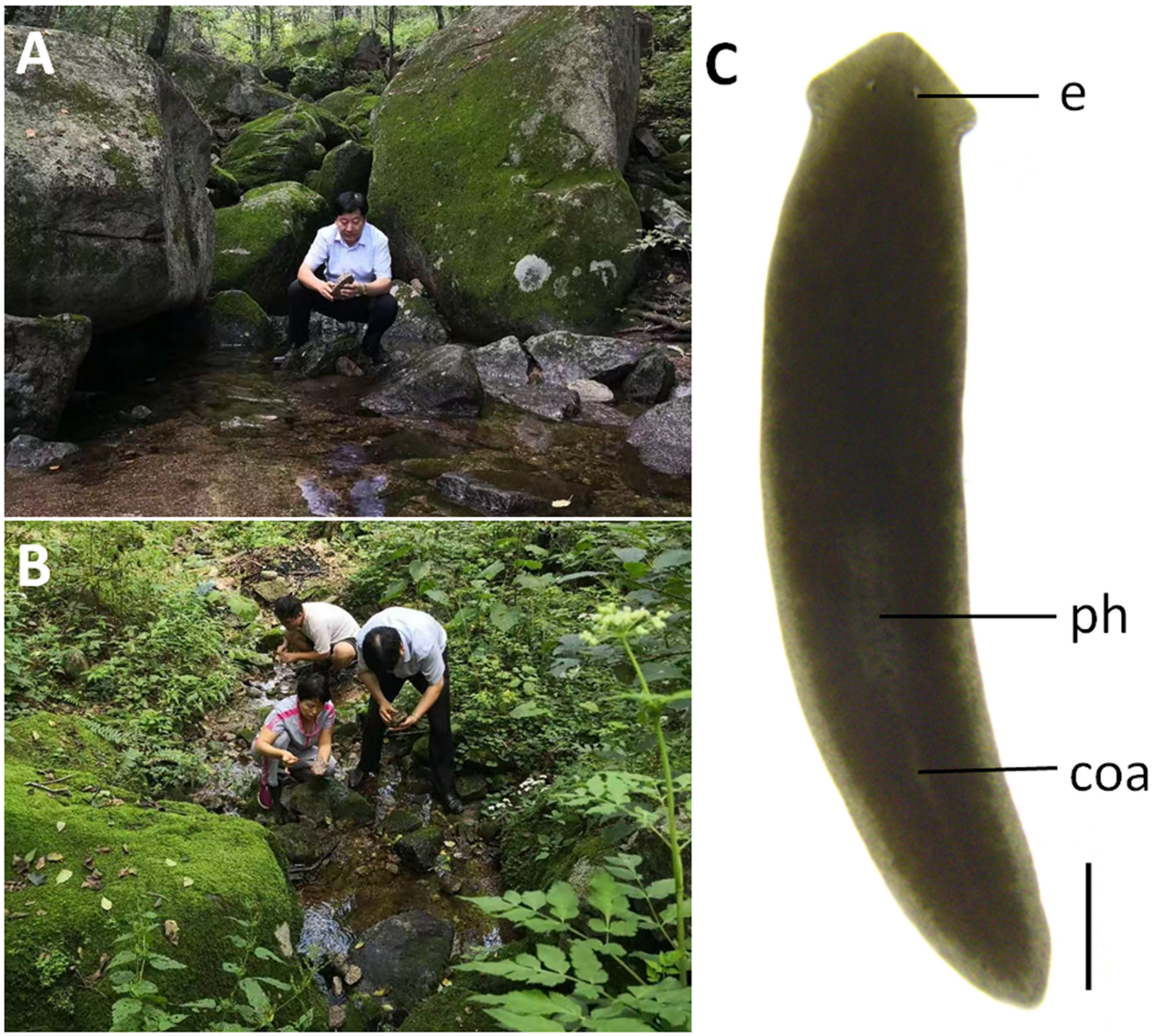

Figure 9. Habitat and external appearance of *Dugesia elongata*. **A, B.** Sampling site and habitat; the person in panel **A** is a co-author of the present paper, Professor Guang-Wen Chen; **C.** Sexually mature, live individual. Scale bar: 2 mm.

water temperature of 6 °C (Figs 1, 9A, B). The water was clear and flowed slowly. At collection, individual worms were large, while mayfly larvae were present in the water.

Material examined. ***Holotype*****:** •ZMHNU—JJM8, Baiyun Mountain in Song village (33°54'43"N, 111°83'49"E; alt. 1100 m a.s.l.), Luoyang County, Henan Province, China, 25 October 2021, coll. G-W. Chen, Z-M. Dong and co-workers, sagittal sections on 36 slides.

Paratypes**:** •ZMHNU—JJM 1, 2, 4, 8, ibid., sagittal sections on 39, 55, 65, and 55 slides, respectively; •ZMHNU—JJM 6, 7, 10, ibid., horizontal sections on 32, 16, and 29 slides; •ZMHNU—JJM 3 and 11, ibid., transverse sections on 49 and 51 slides, respectively. •RMNH.VER.22730.1, ibid., sagittal sections on 41 slides; •RMNH.VER.22730.2, ibid., sagittal sections on 32 slides.

Other material**:** •ZMHNU—SYXKZ1-3, Shuiyunxuan pub Yangcheng village (35°21'29"N, 112°11'1"E; alt. 1150 m a.s.l.), Jincheng City, Shanxi Province, sagittal sections on 15, 14, and 15 slides, respectively. •RMNH.VER.22731.1, ibid., sagittal sections on 10 slides.

Diagnosis. *Dugesia elongata* is characterized by the presence of the following features: relatively large worms; plump, barrel-shaped penis papilla; presence of an elongated, dumb-bell-shaped seminal vesicle; a well-developed connecting duct extending from the seminal vesicle and communicating with a low-conical diaphragm; ventrally displaced ejaculatory duct opening at the tip of the penial papilla, albeit at its ventral portion; asymmetrical openings of the oviducts, with the left oviduct opening into the ventral portion of the common atrium and the right oviduct opening into the bursal canal; copulatory bursa located at a short distance (approximately 487–696 μm) behind the pharyngeal pocket.

Etymology. The specific epithet is derived from the Latin *elongatus*, having been stretched out, extended, and alludes to the long and dumb-bell-shaped seminal vesicle.

Karyology. Eight intact specimens were randomly selected to prepare metaphase plates. A total of 185 metaphase plates were examined, in which 83 plates exhibited diploid chromosome complements of $2n = 2x = 16$,

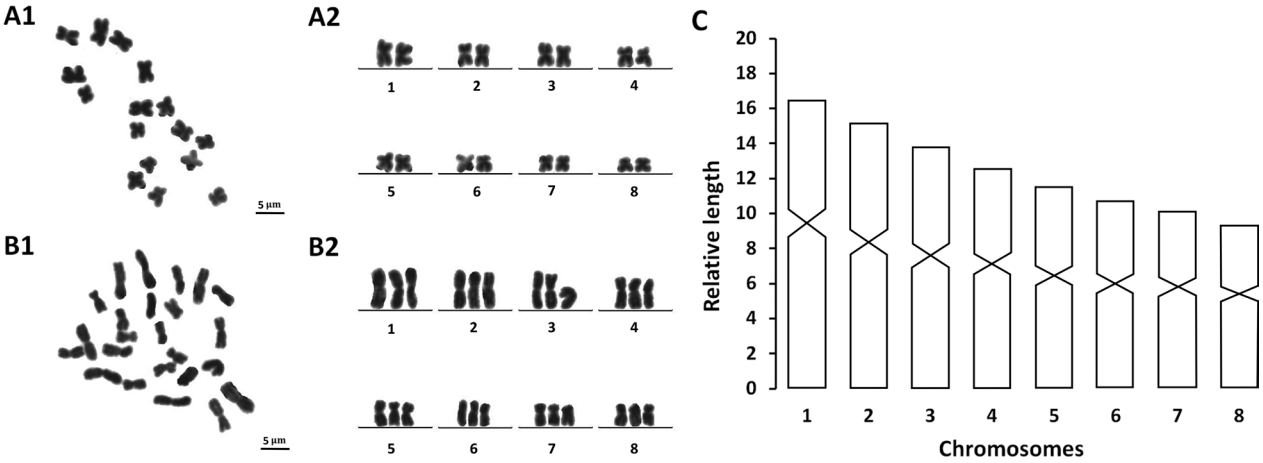

Figure 10. *Dugesia elongata*. **A1, A2.** Metaphase plate and karyogram of diploid complement; **B1, B2.** Metaphase plate and karyogram of triploid complement; **C.** Idiogram. Scale bar: 5 µm.

while in 102 plates, chromosome complements were triploid with $2n = 3x = 24$ chromosomes. All eight specimens exhibited mixoploid chromosome complements, and all chromosomes were metacentric. Karyotype parameters, including relative length, arm ratio, and centromeric index, are given in Table 3. Chromosomal plates and the idiogram are shown in Fig. 10.

Description. The animals were rather large, and most of them were sexually mature. The asexual animals measured 15–30 mm in length and 1.8–3.8 mm in width, while the sexual worms were 25–38 mm in length and 2.8–3.9 mm in width. The low-triangular head is provided with two blunt auricles and two eyes, which are placed in pigment-free patches (Fig. 9C). Each pigmented eyecup houses numerous photoreceptor cells. The dorsal surface is black-brown, except the pale, broad margin of the body; the ventral surface shows a brown hue, which is paler than the dorsal colouration.

Pharynx situated in the posterior region of the body, measuring approximately 1/7th of the body length (Fig. 9C). Mouth opening located at the posterior end of the pharyngeal pocket. Outer pharyngeal muscle layer is composed of a subepithelial, thin layer of longitudinal muscles, followed by a thin layer of circular muscles; no extra inner layer of longitudinal muscles was observed. The inner pharyngeal musculature consists of a subepithelial, thick layer of circular muscle, followed by a thin layer of longitudinal muscle.

In all specimens in which the ovaries could be examined (JJM-5, 8, 9), the gonads were hyperplasic, occupying 1/3–2/3 of the dorsoventral space The oviducts extend from the dorsal wall of the ovaries and run to the posterior part of the body, and when posteriorly to the gonopore, they curve dorsally and also recurve and then open asymmetrically into the copulatory apparatus (Fig. 11B). The right oviducal opening is higher than the left one, in that it is located at the point where the bursal canal communicates with the common atrium. The left oviduct opens into the lower, ventral portion of the common atrium. Cyanophil shell glands discharge their secretion into the vaginal region of the bursal canal, at the level of the oviducal openings.

The large and sac-shaped copulatory bursa is situated at a short distance behind the pharyngeal pocket, ranging between approximately 487–696 µm in all specimens in which it could be measured (JJM-2, 4, 5, 8, 9). The bursa is a large and oblong, sac-like structure that occupies the entire dorso-ventral space, and is twice as long as it is high. Its lining consists of columnar, vacuolated cells with basal nuclei.

The bursal canal arises from the postero-dorsal wall of the bursa and then expands in diameter to become a wide duct. At the level of the gonopore the bursal canal makes a knee-shaped bend towards the ventral body surface to connect with the common atrium. The bursal canal is lined with a ciliated epithelium with basal nuclei.

Table 3. Karyotype parameters (mean values and standard deviations) of *Dugesia elongata* Chen & Dong, sp. nov.; m, metacentric.

Chromosome	Relative length	Arm ratio	Centromeric index	Chromosome type
1	1.65 ± 0.95	1.37 ± 0.38	44.01 ± 2.03	m
2	15.23 ± 0.94	1.23 ± 0.17	45.19 ± 3.00	m
3	13.73 ± 0.57	1.26 ± 0.13	44.53 ± 2.51	m
4	12.65 ± 0.59	1.31 ± 0.16	43.74 ± 2.92	m
5	11.54 ± 0.67	1.29 ± 0.13	43.97 ± 2.49	m
6	10.75 ± 0.52	1.28 ± 0.19	44.03 ± 3.59	m
7	10.17 ± 0.76	1.41 ± 0.28	42.82 ± 2.81	m
8	9.39 ± 0.50	1.39 ± 0.26	42.55 ± 4.26	m

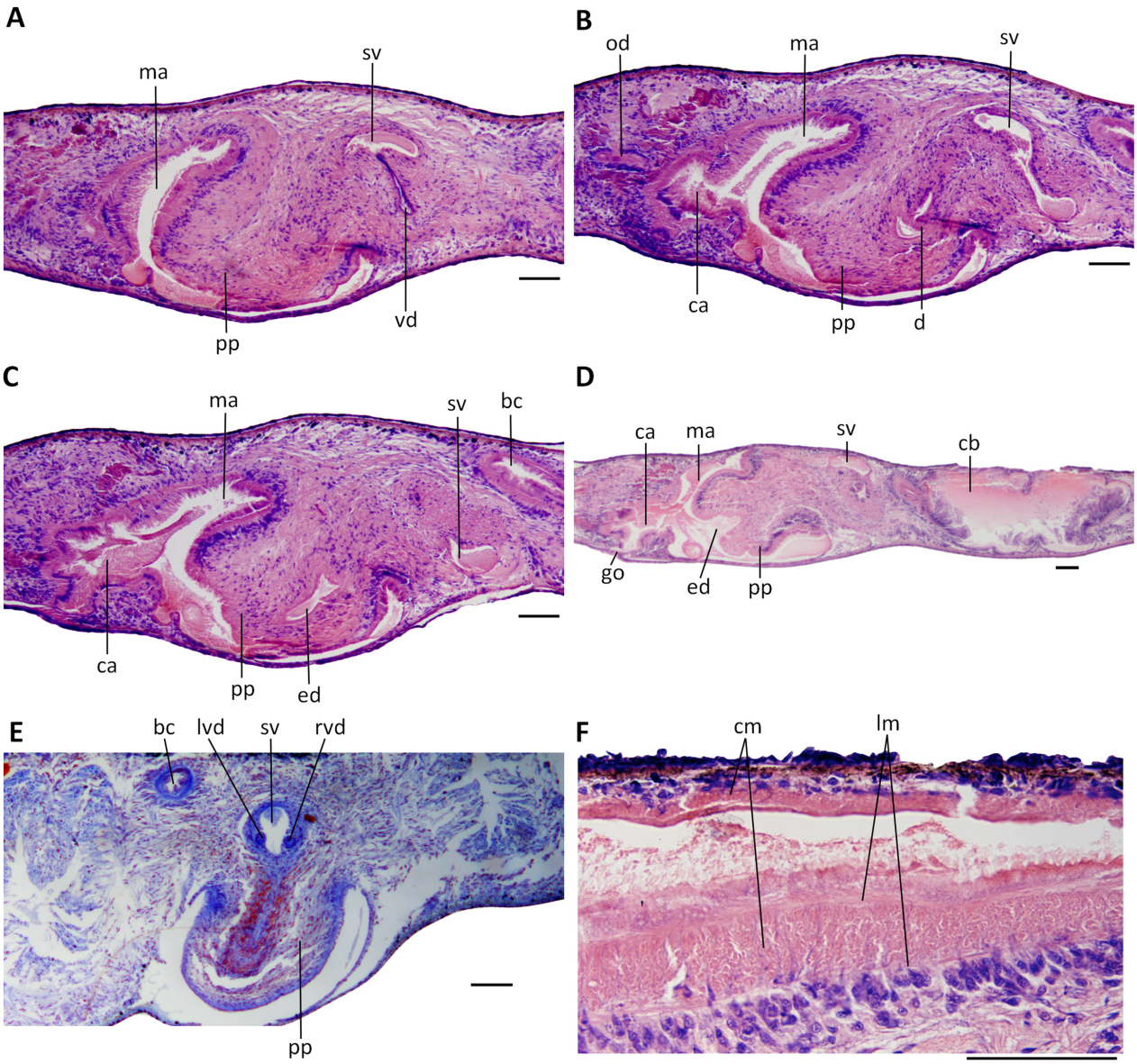

Figure 11. *Dugesia elongata*. Photomicrographs. **A.** Sagittal section of holotype JJM8, showing penis papilla and vas deferens opening into the seminal vesicle; **B.** Sagittal section of holotype JJM8, showing penis papilla, seminal vesicle, diaphragm, oviduct, male atrium, and common atrium; **C.** Sagittal section of holotype JJM8, showing penis papilla, seminal vesicle, ejaculatory duct, male atrium, and common atrium; **D.** Sagittal section of paratype JJM9, showing copulatory bursa, seminal vesicle, penis papilla, male atrium, common atrium, gonopore, and opening of ejaculatory duct; **E.** Transverse section of paratype JJM11, showing seminal vesicle and symmetrical openings of the vasa deferentia into the seminal vesicle; **F.** Sagittal section of paratype JJM9, showing musculature of the bursal canal. Scale bars: 100 μm.

It is surrounded by three layers of muscle, the innermost layer being a thin layer of longitudinal muscles, the middle layer a slightly thicker layer of circular muscle, followed by a thin outermost layer of longitudinal muscles, which forms the ectal reinforcement layer and extends from the atrium to approximately 4/5 of the length of the bursal canal. The circular muscle layer is relatively thick along the ventral wall of the bursal canal but much thinner along its dorsal wall.

In all specimens in which the testes could be examined (except JJM-4), the well-developed, albeit small, follicles are located on the dorsal side and extend from directly behind the ovaries to the posterior end of the body. At the level of the pharyngeal pocket, in several specimens (except JJM-4), the vasa deferentia expand to form spermiducal vesicles, which are packed with sperm.

The barrel-shaped penis papilla is asymmetrical, in that the ejaculatory duct is ventrally displaced, opening at the tip of the papilla. The penis papilla is covered with a nucleated epithelium, which is underlain by a subepithelial layer of circular muscle, followed by a layer of longitudinal muscle fibers. A major portion of the dorsal wall of the penis papilla receives the openings of erythrophil glands, while a smaller part on its ventral wall is penetrated by openings of similar glands.

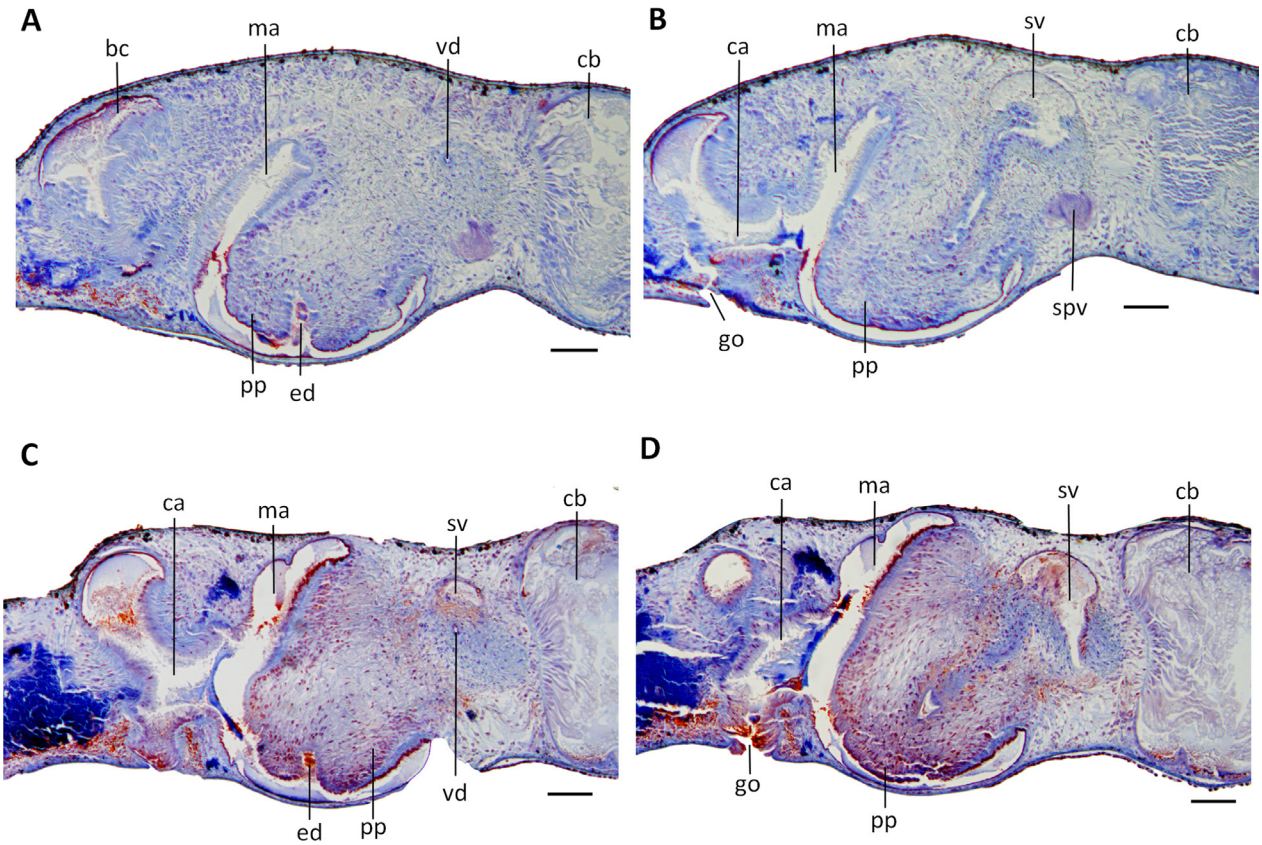

Figure 12. *Dugesia elongata*. Photomicrographs of sagittal sections. **A.** Specimen SYXKZ1, showing penis papilla, vas deferens, openings of ejaculatory duct, male atrium, copulatory bursa, and bursal canal; **B.** Specimen SYXKZ1, showing penis papilla, seminal vesicle, copulatory bursa, spermiducal vesicle, male atrium, common atrium, and gonopore; **C.** Specimen RMNH.VER.22731.1, showing penis papilla, seminal vesicle, vas deferens, openings of ejaculatory duct, male atrium, common atrium, and copulatory bursa; **D.** Specimen RMNH.VER.22731.1, showing copulatory bursa, seminal vesicle, penis papilla, male atrium, common atrium, and gonopore. Scale bars: 100 µm.

The penis bulb is lopsided, with its antero-ventral portion being near the ventral epidermis. That portion of the penis bulb houses the ventro-anterior portion of the seminal vesicle, which at its dorsal side narrows into a canal that runs anterodorsally and opens into another, again expanded portion of the seminal vesicle. Consequently, the seminal vesicle has the shape of a dumb-bell. The seminal vesicle is lined by a flat, nucleated epithelium and is surrounded by a layer of intermingled muscle fibers. The dorsally located portion of the dumb-bell symmetrically receives at its mid-ventral section the separate openings of the highly narrowed vasa deferentia, which are surrounded by a layer of circular muscles.

The anterior wall of the dorsally located portion of the seminal vesicle continues into a relatively long connecting duct that curves antero-ventrad and opens into a low-conical diaphragm, which opens into the ejaculatory duct. The diaphragm and the ejaculatory duct receive the abundant secretion of erythrophil penis glands (Figs 11B, 13).

The genital cavity is divided into a common atrium and a male atrium, which communicate through a relatively narrow canal. The common atrium communicates with the bursal canal and also leads to the gonopore, which receives the openings of a large number of cement glands (Figs 11B–D, 13).

In several specimens, a spermatophore protruded from the opening of the ejaculatory duct at the tip of the penis papilla.

Reproduction. After 4 months of laboratory culturing, the asexual specimens continuously sexualized and produced cocoons. After approximately 20 days, five juveniles hatched from these cocoons. However, from then on, none of the worms produced any more cocoons.

Discussion. The specimens from the other locality are consistent with those from the holotype site (Fig. 12). The coexistence of a long, dumb-bell-shaped seminal vesicle, a diaphragm, and a duct is found in only two *Dugesia* species, *D. saccaria* and *D. verrucula*. However, *D. elongata* cannot be synonymized with either of these two species. *Dugesia saccaria* has a dumbbell-shaped, muscularized hump located just anterior to the knee-shaped bend in the bursal canal. In addition, the ejaculatory duct opens terminally through the dorsal portion of the blunt tip of the penis papilla (Zeng et al. 2024), which contrasts with the ventral opening in *D. elongata*. *Dugesia verrucula* also has a dumbbell-shaped seminal vesicle surrounded by distinct

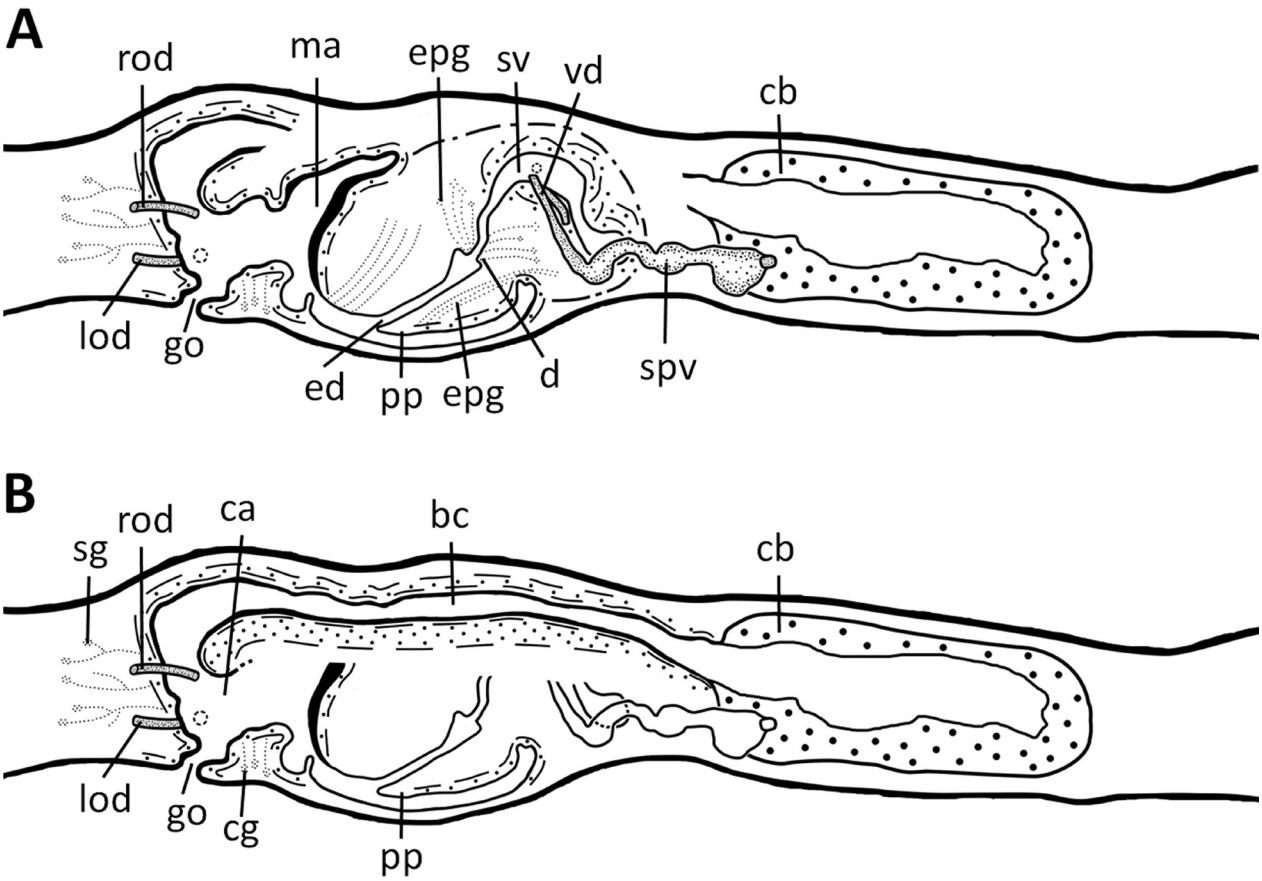

Figure 13. *Dugesia elongata*. Sagittal reconstruction of the copulatory apparatus of holotype JJM8. **A.** Sagittal reconstruction of female copulatory apparatus; **B.** Sagittal reconstruction of male copulatory apparatus. Scale bar: 100 μm.

musculature, like *D. elongata*. Unfortunately, this was not properly described by Wang et al. (2021a), and it was also incorrectly described that in *D. verrucula*, the ejaculatory duct arises from the dorsal portion of the seminal vesicle. However, the ejaculatory duct always arises after, i.e., distally to the diaphragm. There is a difference, in that in *D. verrucula*, the vasa deferentia open into the proximal portion of the dumb-bell, whereas in *D. elongata*, the ducts open into the distal part of the dumb-bell-shaped seminal vesicle. However, the most characteristic feature of *D. verrucula* is the permanent dorsal bump on its penis papilla, which is absent in *D. elongata* (Wang et al. 2021a).

In addition, *D. elongata*, *D. verrucula*, and *D. constrictiva* also belong to a small clade in the phylogenetic tree (Fig. 2). However, *D. elongata* and *D. constrictiva* are anatomically rather different (Wang et al. 2022). *Dugesia constrictiva* has a laterally compressed seminal vesicle and a cuboidal copulatory bursa, which are different from the elongated, dumb-bell-shaped seminal vesicle and the oblong, sac-like copulatory bursa of *D. elongata*. Furthermore, *D. verrucula* and *D. constrictiva* exhibit a diploid chromosome complement of $2n = 2x = 16$, with a haploid number of $n = 8$, in contrast to the chromosome portrait of *D. elongata*, which shows a mixoploid karyotype with diploid complements of $2n = 2x = 16$ and triploid sets of $2n = 3x = 24$. The lowest *COI* and *ITS-1* distance values between *D. elongata* and its congeners were 12.02% (*D. elongata* with *D. constrictiva*) and 1.66% (*D. elongata* with *D. verrucula*), respectively. Therefore, *D. elongata* is well separated from its congeners, which further supports its separate specific status as suggested by the anatomical and karyological analyses.

General discussion

Phylogeny

The topology of the phylogenetic tree (Fig. 2) is basically consistent with previous phylogenetic analyses, except for some nodes (Lázaro et al. 2009; Solà et al. 2013; Stocchino et al. 2017; Song et al. 2020). Previous studies showed that the lowest distances for *COI* between species are commonly greater than 6%, and those for *ITS-1* between species are usually more than 1% (Lázaro et al. 2009; Solà et al. 2013; Stocchino et al. 2017). These values are surpassed by the genetic distances determined for *D. elongata*, which thus support the results of the morphological and phylogenetic analyses. Despite the fact that *D. cylindrica* has a relatively low genetic distance to *D. patula* and shares with the latter many anatomical features, the phylogenetic analysis and the molecular species delimitation suggest that they are different species. Anatomically, these two sibling species differ only in the position of the copulatory bursa,

which is located at some distance behind the pharyngeal pouch in *D. patula*, whereas in *D. cylindrica*, it is positioned immediately behind the pharyngeal pocket.

The phylogenetic relationships revealed in this study provide significant insights into the biogeographical history of the genus *Dugesia* in northern China. The analyses robustly place the two newly described species within distinct subclades of the Eastern Palearctic/Oriental/Australasian group. *Dugesia cylindrica* shares a sister-group relationship (Fig. 2; pp = 1.00, bs = 100) with a small clade comprising *D. patula* and *D. postica* (Fig. 2; pp = 0.82, bs = 77), two *Dugesia* species recently described from the Hengduan Mountains in southern China (Wu et al. 2025). The Hengduan Mountains and Taihang Mountains are separated by the continuous mountain barrier of the Qinling Mountains and the vast lowlands of the North China Plain, the Loess Plateau, and the plain of the middle and lower reaches of the Yangtze River (Zhao et al. 2012; Sun et al. 2024). These areas constitute significant geographical barriers, especially for species with weak dispersal capacity. How these two species spread and diverged is worth studying. *Dugesia elongata* is sister to *D. constrictiva* (Fig. 2; pp = 1.00, bs = 94), which was also described from the Taihang Mountains (Wang et al. 2022). Together, they are sisters to *D. verrucula* (Fig. 2; pp = 1.00, bs = 100) from the Shiwan Dashan Mountain National Natural Reserve in Guangxi Province (Wang et al. 2021a). This close phylogenetic affinity suggests a historical connection between the biotas of northern and southern China, with the present-day disjunct distribution potentially reflecting past biogeographical events.

Distribution and ecology

A finding of this study is the confirmation that *D. cylindrica* was recorded from multiple localities spanning the southern Taihang Mountains, while *D. elongata* was found in both the Funiu Mountains and a locality in the Taihang Mountains (Fig. 1). The fact that two new species were found at multiple locations suggests that this region is a significant reservoir of freshwater planarian diversity. The complex topography, abundant water resources, and temperate monsoon climate of these mountains have created a mosaic of stable freshwater habitats that have facilitated both the speciation and dispersal of these taxa. Up to now, only one *Dugesia* species has been reported from northern China, viz., *D. constrictiva* from the Taihang Mountains (Wang et al. 2022). Previously, four species of the planarian genus *Polycelis* Ehrenberg, 1831 have been reported (Liu 1996; Chen et al. 2008; Dong et al. 2017). The discovery of two species in a region previously thought to harbor limited diversity strongly supports the hypothesis that the Palearctic Realm of China is a potential hotspot for *Dugesia* and that its species richness has been underestimated.

In addition, the low water temperature recorded for *D. elongata* perhaps reflects the complex interplay of seasonal sampling timing, spring-fed habitat characteristics, and genuine physiological adaptation to cool environments. It is the lowest documented temperature for any Chinese *Dugesia* species to date. The collection site for *D. elongata* is a spring. Unlike open streams that are more susceptible to ambient temperature fluctuations, spring systems maintain relatively constant, cool temperatures throughout the year. Furthermore, species at equivalent springs elsewhere have also been recorded from cool waters, such as *D. cretica* (Meixner, 1928) (Dahm 1958). Notably, the latter collection latitude is considerably higher than that of Hainan Island and the Leizhou Peninsula, while the water temperature and air temperature in the Funiu Mountains are relatively low (Wang et al. 2025). Temperature has been shown to regulate the switch between asexual and sexual reproduction in planarians. Low temperatures usually promote sexual reproduction, while high temperatures favor asexual fission (Vowinckel and Marsden 1971). Both the ability of *D. elongata* to maintain sexual reproduction at 6 °C and the laboratory-induced sexualization of warm-adapted Hainan species at lower temperatures support this mechanism (Wang et al. 2021b). Therefore, water temperature is hypothesized to be a key factor in shaping the diversity and composition of *Dugesia* species in Chinese mountains.

Karyological diversity

The genus *Dugesia* exhibits remarkable chromosomal diversity; its haploid chromosome sets were always classified into three karyological groups: $n = 7$, $n = 8$, and $n = 9$ (Ball 1970). Recently, the discovery of a Madagascan population with a diploid complement of $2n = 10$ ($n = 5$) represents the lowest chromosome number ever recorded for the genus, establishing a fourth karyological group (Stocchino et al. 2024). This finding underscores that the haploid complements of $n = 5$ and $n = 9$ were already present in ancestral *Dugesia* species and that the two other karyological groups ($n = 7$ and $n = 8$) originated through chromosomal rearrangements. In Chinese *Dugesia* species, the majority possess a haploid chromosome number of $n = 8$, while a few exhibit $n = 7$ (Chen et al. 2022; Wang et al. 2025). The $n = 9$ karyological group has not yet been recorded from China, and it is exhibited only by one species from Yemen, four species from the Afrotropical region, and two species from the Mediterranean region (Stocchino et al. 2024).

Polyploidy and mixoploidy, as in *D. elongata*, are particularly prevalent in asexually reproducing populations and have profound ecological implications. It has been proposed that a mixoploid karyotype serves as an adaptive mechanism to withstand harsh environmental conditions, such as high temperatures and intense solar radiation (Stocchino et al. 2004; Harrath et al. 2025). In addition, several species exhibit the presence of B chromosomes. *Dugesia pendula* from southern China shows an aneuploid plus mixoploid karyotype with diploid ($2n = 14 + 0–1$ B) and triploid ($2n = 21 + 0–1$ B) sets. The species reproduces asexually in nature while retaining the capacity for sexual development under laboratory culture (Wang et al. 2024). Apart from the

situation in *D. pendula*, the condition of aneuploidy has also been reported for several other species of *Dugesia*, such as *D. ryukyuensis* Kawakatsu, 1976, *D. japonica*, and *D. arabica* Harrath & Sluys, 2013. This adds another layer of karyological complexity, with their numbers sometimes varying along environmental gradients, suggesting possible adaptive functions (Oki et al. 1981; Harrath et al. 2013). This karyological perspective reveals that chromosomal diversification, including polyploidy, aneuploidy, and supernumerary elements, probably constitutes a critical but often overlooked dimension of planarian biodiversity, shaping not only evolutionary trajectories but also ecological adaptations and reproductive strategies across the genus.

Uncovering cryptic diversity

The present case of the two sibling species *D. cylindrica* and *D. patula* has been preceded by earlier examples of cryptic diversity in the genus *Dugesia*. For example, *D. benazzii* Lepori, 1951 was thought to be distributed across the Mediterranean islands of Corsica and Sardinia, a notion that was challenged when detailed studies revealed the presence of species such as *D. hepta* Pala, Casu & Vacca, 1981, *D. leporii* Pala, Stocchino, Corso & Casu, 2000, *D. sicula* Lepori, 1948, *D. mariae* Stocchino, Dols-Serrate & Riutort, 2024, *D. hoidi* Dols-Serrate, Stocchino & Riutort, 2024, and *D. xeropotamica* Stocchino, Dols-Serrate & Riutort, 2024. Although these species are not well separated by genetic distance for *COI*, they can be well differentiated by means of molecular species delimitation (Dols-Serrate et al. 2020, 2024a, 2024b). Similarly, *D. aethiopica* Stocchino, Corso, Manconi & Pala, 2002 from Ethiopia and *D. arabica* from Yemen cannot be separated by genetic distance for *COI* (Harrath et al. 2013). All of these results indicate that DNA barcoding fails in special cases, such as cryptic species and closely related species. Thus, these species can be distinguished only through an integrative approach, using both anatomical and molecular species delimitation. In recent years, molecular species delimitation has also played an important role in the analysis of cryptic *Dugesia* species from the Mediterranean Sea and continental Europe (Leria et al. 2020; Dols-Serrate et al. 2024a, 2024b).

Funding

This work was supported by the National Natural Science Foundation of China (grant numbers: 32270501, 32470463); the Foundation for the Key Research Program of Higher Education of Henan Province (25A180017); Postdoctoral Research Project of Henan Province (grant numbers: HN2022136, HN2025018); the Natural Science Foundation of Henan Province (grant number: 242300420495); the Major Public Welfare Project of Henan Province (grant number: 201300311700); and the Puyang Field Scientific Observation and Research Station for Yellow River Wetland Ecosystem, Henan Provinc.

Author contributions

Guang-Wen Chen and Zi-Mei Dong conceived and designed the study. Guang-Wen Chen, Zi-Mei Dong, Lei Wang, and Fan Wu sampled the specimens. Yi-Fan Su, Lei Wang, Fan Wu, and Fu-Yu Yu made the histological sections. Guang-Wen Chen, Zi-Mei Dong, Lei Wang, De-Zeng Liu, Ronald Sluys, and Yi-Fan Su analyzed the histological sections. Lei Wang prepared the reconstruction drawings. Lei Wang and Yi-Fan Su prepared and examined metaphase plates. Lei Wang, Fan Wu, Jing-Yi Wang, and Yi-Fan Su performed the molecular analyses. Yi-Fan Su wrote the first draft of the manuscript. Guang-Wen Chen, Zi-Mei Dong, Ronald Sluys, and Lei Wang reviewed, revised, and finalized the manuscript. All authors read and approved the final manuscript.

Conflicts of interest

The authors declare that they have no conflicts of interest.

Ethics approval and consent to participate

All handling procedures were strictly compliant with the current Animal Protection Law of China. This study did not involve endangered or protected species. No approvals were required for collections of specimens from the locations in this study. Ethical approval was not required at Henan Normal University, Xinxiang University, or Naturalis Biodiversity Center for research conducted on invertebrates such as flatworms used in this study.

Acknowledgments

The authors are grateful to Dr. Eduard Solà (Universitat de Barcelona) for his insightful comments on the molecular analyses in an earlier version of the manuscript.

References

Abascal F, Zardoya R, Telford MJ (2010) TranslatorX: Multiple alignment of nucleotide sequences guided by amino acid translations. Nucleic Acids Research 38 (suppl. 2): W7–13. https://doi.org/10.1093/nar/gkq291

Ball IR (1970) Freshwater triclads (Turbellaria, Tricladida) from the Oriental region. Zoological Journal of the Linnean Society 49(4): 271–294. https://doi.org/10.1111/j.1096-3642.1970.tb00742.x

Chen G-W, Wang L, Wu F, Sun X-J, Dong Z-M, Sluys R, Yu F, Yu-wen Y-Q, Liu D-Z (2022) Two new species of *Dugesia* (Platyhelminthes, Tricladida, Dugesiidae) from the subtropical monsoon region in Southern China, with a discussion on reproductive modalities. BMC Zoology 7(1): 25. https://doi.org/10.1186/s40850-022-00127-8

Chen G-W, Wang Y-L, Wang H-K, Fu R-M, Zhang J-F, Liu D-Z (2008) Chromosome and karyotype analysis of *Polycelis wutaishanica* (Turbellaria, Tricladida) from Shanxi province,

China. Acta Zootaxonomica Sinica 33(3): 449–452. https://doi.org/10.1186/1471-2164-13-290

Dahm AG (1958) Taxonomy and ecology of five species groups in the family Planariidae (Turbellaria Tricladida Paludicola). Malmö: Nya Litografen, 241 pp.

Dessimoz C, Gil M (2010) Phylogenetic assessment of alignments reveals neglected tree signal in gaps. Genome biology 11(4): R37. https://doi.org/10.1186/gb-2010-11-4-r37

Dols-Serrate D, Leria L, Aguilar JP, Stocchino GA, Riutort M (2020) *Dugesia hepta* and *Dugesia benazzii* (Platyhelminthes: Tricladida): two sympatric species with occasional sex? Organisms Diversity and Evolution 20: 369–386. https://doi.org/10.1007/s13127-020-00438-z

Dols-Serrate D, Stocchino GA, Sluys R, Riutort M (2024a) Fantastic beasts and how to delimit them: an integrative approach using multispecies coalescent methods reveals two new, endemic *Dugesia* species (Platyhelminthes: Tricladida) from Corsica and Sardinia. Zoological Journal of the Linnean Society 201(3): zlad135. https://doi.org/10.1093/zoolinnean/zlad135

Dols-Serrate D, Stocchino GA, Nuin-Villabona P, Sluys R, Riutort M (2024b) New insights into the evolution and biogeography of freshwater planarians on islands in the Tyrrhenian Sea, Western Mediterranean Basin, with the integrative description of a new endemic species from Corsica (Platyhelminthes: Tricladida: *Dugesia*). Zoological Journal of the Linnean Society 201(4): zlae080. https://doi.org/10.1093/zoolinnean/zlae080

Dong Z-M, Chen G-W, Zhang H-C, Liu D-Z (2017) A new species of *Polycelis* (Platyhelminthes, Tricladida, Planariidae) from China. Acta Zoologica Academiae Scientiarum Hungaricae 63(3): 263–276. https://doi.org/10.17109/AZH.63.3.263.2017

Dong Y-P, Shi X-H, Sun S-S, Sun J-P, Hui B, He D-F, Chong F-B, Yang Z (2022) Co-evolution of the Cenozoic tectonics, geomorphology, environment and ecosystem in the Qinling Mountains and adjacent areas, Central China. Geosystems and Geoenvironment 1(2): 100032. https://doi.org/10.1016/j.geogeo.2022.100032

Hall FR (1999) Precision farming: Technologies and information as risk-reduction tools. Nucleic Acids Symposium Series, vol. 734, no. 41, pp. 95–98. https://doi.org/10.1021/bk-1999-0734.ch008

Harrath AH, Sluys R, Aldahmash W, Al-Razaki A, Alwasel S (2013) Reproductive strategies, karyology, parasites, and taxonomic status of *Dugesia* populations from Yemen (Platyhelminthes: Tricladida: Dugesiidae). Zoological Science 30(6): 502-508. https://doi.org/10.2108/zsj.30.502

Harrath AH, Mansour L, Sluys R, Aldahmash W, Riutort M, Alwasel S (2025) The first *Dugesia* species (Platyhelminthes, Tricladida, Dugesiidae) documented for Saudi Arabia: an integrative description. Zootaxa 5583(1): 113–127. https://doi.org/10.11646/zootaxa.5583.1.6

Katoh K, Standley D-M (2013) MAFFT multiple sequence alignment software version 7: improvements in performance and usability. Molecular Biology and Evolution 30(4): 772–780. https://doi.org/10.1093/molbev/mst010

Kawakatsu M (1968) On the origin and phylogeny of Turbellarians Suborder Paludicola. Japanese Society of Systematic Zoology, Circular no. 38–41: 11–22. [in Japanese]

Lanfear R, Calcott B, Ho S-Y, Guindon S (2012) PartitionFinder: combined selection of partitioning schemes and substitution models for phylogenetic analyses. Molecular Biology and Evolution 29(6): 1695–1701. https://doi.org/10.1093/molbev/mss020

Lanfear R, Frandsen P-B, Wright A-M, Senfeld T, Calcott B (2017) PartitionFinder 2: new methods for selecting partitioned models of evolution for molecular and morphological phylogenetic analyses. Molecular Biology and Evolution 34(3): 772–773. https://doi.org/10.1093/molbev/msw260

Lázaro E-M, Sluys R, Pala M, Stocchino G-A, Baguñà J, Riutort M (2009) Molecular barcoding and phylogeography of sexual and asexual freshwater planarians of the genus *Dugesia* in the Western Mediterranean (Platyhelminthes, Tricladida, Dugesiidae). Molecular Phylogenetics and Evolution 52: 835–845. https://doi.org/10.1016/j.ympev.2009.04.022

Leria L, Vila-Farré M, Álvarez-Presas M, Sánchez-Gracia A, Rozas J, Sluys R, Riutort M (2020) Cryptic species delineation in freshwater planarians of the genus *Dugesia* (Platyhelminthes, Tricladida): Extreme intraindividual genetic diversity, morphological stasis, and karyological variability. Molecular Phylogenetics and Evolution 143: 106496. https://doi.org/10.1016/j.ympev.2019.05.010

Levan A, Fredga K, Sandberg A-A (1964) Nomenclature for centromeric position on chromosomes. Hereditas 52: 201–220. https://doi.org/10.1111/j.1601-5223.1964.tb01953.x

Li J-K, Peng J-F, Wei X-X, Peng M, Li X, Liu Y-M, Li J-X (2024) Stability assessment of tree ring growth of *Pinus armandii* Franch in response to climate change based on slope directions at the Lubanling in the Funiu Mountains, China. Journal of Forestry Research 35(03): 88–99. https://doi.org/10.1007/s11676-024-01698-7

Li X-N, Huo J-X, Yang L, Peng J-F (2020) Development and climatic response of the tree-ring width chronology of *Pinus armandii* at Muzhaling Mountain. Journal of Nanjing Forestry University 44(3): 157–162. https://doi.org/10.3969/j.issn.1000-2006.201901030

Liu D-Z (1996) Notes on four new species of the genus *Polycelis* from China (Tricladida: Paludicola: Planariidae). Acta Zootaxonomica Sinica 21(4): 389–398. [in Chinese] https://doi.org/10.3724/issn1000-3207-1995-2-152-c

Mo R-R, Yan Y-H, Wang G-Q, Li W-H, Murányi D (2019) Holomorphology of *Kamimuria peppapiggia* sp. n. (Plecoptera: Perlidae) from the foothills of Taihang Mountains, Henan Province of China. Zootaxa 4668(4): 575–587. https://doi.org/10.11646/zootaxa.4668.4.9

Oki I, Tamura S, Yamayoshi T, Kawakatsu M (1981) Karyological and taxonomic studies of *Dugesia japonica* Ichikawa & Kawakatsu in the Far East. Hydrobiologia 84: 53–68. https://doi.org/10.1007/bf00026163

Puillandre N, Brouillet S, Achaz G (2021) ASAP: Assemble Species by Automatic Partitioning. Molecular Ecology Resources 21(2): 609–620. https://doi.org/10.1111/1755-0998.13281

Puillandre N, Lambert A, Brouillet S, Achaz G (2011) ABGD, Automatic Barcode Gap Discovery for Primary Species Delimitation. Molecular Ecology 21(8): 1864–1877. https://doi.org/10.1111/j.1365-294X.2011.05239.x

Rambaut A, Drummond A-J, Xie D, Baele G, Suchard M-A (2018) Posterior summarization in Bayesian Phylogenetics Using Tracer 1.7. Systematic Biology 67(5): 901–904. https://doi.org/10.1093/sysbio/syy032

Ronquist F, Teslenko M, van der Mark P, Ayres D-L, Darling A, Höhna S, Larget B, Liu L, Suchard M-A, Huelsenbeck J-P (2012) MrBayes 3.2: efficient Bayesian phylogenetic inference and model choice across a large model space. Systematic Biology 61: 539–542. https://doi.org/10.1093/sysbio/sys029

Sluys R, Kawakatsu M, Winsor L (1998) The genus *Dugesia* in Australia, with its phylogenetic analysis and historical biogeography (Platyhelminthes, Tricladida, Dugesiidae). Zoologica Scripta 27(4): 273–289. https://doi.org/10.1111/j.1463-6409.1998.tb00461.x

Sluys R, Riutort M (2018) Planarian diversity and phylogeny. In: Rink JC (ed.), Planarian Regeneration: Methods and Protocols. Methods in Molecular Biology, vol. 1774, Humana Press,

Springer Science+Business Media. New Yrok, 1–56. https://doi.org/10.1007/978-1-4939-7802-1

Sluys R, Sola E, Gritzalis K, Vila-Farre M, Mateos E, Riutort M (2013) Integrative delineation of species of Mediterranean freshwater planarians (Platyhelminthes: Tricladida: Dugesiidae). Zoological Journal of the Linnean Society 169(3): 523–547. https://doi.org/10.1111/zoj.12077

Solà E, Leria L, Stocchino G-A, Bagherzadeh R, Balke M, Daniels S-R, Harrath AH, Khang T-F, Krailas D, Kumar B, Li M-H, Maghsoudlou A, Matsumoto M, Naser N, Oben B, Segev O, Thielicke M, Tong X-L, Zivanovic G, Manconi R, Baguñà J, Riutort M (2022) Three dispersal routes out of Africa: a puzzling biogeographical history in freshwater planarians. Journal of Biogeography 49(7): 1219–1233. https://doi.org/10.1111/jbi.14371

Solà E, Sluys R, Gritzalis K, Riutort M (2013) Fluvial basin history in the northeastern Mediterranean region underlies dispersal and speciation patterns in the genus *Dugesia* (Platyhelminthes, Tricladida, Dugesiidae). Molecular Phylogenetics and Evolution 66: 877–888. https://doi.org/10.1016/j.ympev.2012.11.010

Sun X-X, Wang L, Li N, Sluys R, Liu D-Z, Dong Z-M, Chen G-W (2024) Two species of *Polycelis* (Platyhelminthes, Tricladida, Planariidae) newly recorded for the Qinling Mountains and the Loess Plateau in China, with a comparative discussion on their karyotypes. Zootaxa 5536(4): 581–599. https://doi.org/10.11646/zootaxa.5536.4.5

Song X-Y, Li W-X, Sluys R, Huang S-X, Wang A-T (2020) A new species of *Dugesia* (Platyhelminthes, Tricladida, Dugesiidae) from China, with an account on the histochemical structure of its major nervous system. Zoosystematics and Evolution 96(2): 431–447. https://doi.org/10.3897/zse.96.52484

Stocchino GA, Sluys R, Riutort M, Solà E, Manconi R (2017) Freshwater planarian diversity (Platyhelminthes: Tricladida: Dugesiidae) in Madagascar: new species, cryptic species, with a redefinition of character states. Zoological Journal of the Linnean Society 181: 727–756. https://doi.org/10.1093/zoolinnean/zlx017

Stocchino GA, Manconi R, Corso G, Pala M (2004) Karyology and karyometric analysis of an Afrotropical freshwater planarian (Platyhelminthes, Tricladida). Italian Journal of Zoology 71: 89–93. https://doi.org/10.1080/11250000409356557

Stocchino GA, Sluys R, Solà E, Riutort M, Manconi R (2024) The long-eared freshwater planarians of Madagascar form a separate phylogenetic clade within the genus *Dugesia* (Platyhelminthes: Tricladida), with the description of two new species. Zoological Journal of the Linnean Society 202: zlae143. https://doi.org/10.1093/zoolinnean/zlae143

Talavera G, Castresana J (2007) Improvement of phylogenies after removing divergent and ambiguously aligned blocks from protein sequence alignments. Systematic Biology 56(4): 564–577. https://doi.org/10.1080/10635150701472164

Tamura K, Stecher G, Peterson D, Filipski A, Kumar S (2013) MEGA6: Molecular Evolutionary Genetics Analysis version 6.0. Molecular Biology and Evolution 30: 2725–2729. https://doi.org/10.1093/molbev/mst197

Tan G, Muffato M, Ledergerber C, Herrero J, Goldman N, Gil M, Dessimoz C (2015) Current methods for automated filtering of multiple sequence alignments frequently worsen single-gene phylogenetic inference. Systematic Biology 64(5): 778–791. https://doi.org/10.1093/sysbio/syv033

Vowinckel C, Marsden JR (1971) Reproduction of *Dugesia tigrina* under short-day and long-day conditions at different temperatures. II. Asexually derived individuals. Journal of Embryology and Experimental Morphology 49(5): 659–663. https://doi.org/10.1242/dev.26.3.587

Wang B, Jiang J-P, Xie F, Chen X-H, Dubois A, Liang G, Wagner S (2009) Molecular phylogeny and genetic identification of populations of two species of *Feirana* frogs (Amphibia: Anura, Ranidae, Dicroglossinae, Paini) endemic to China. Zoological Science 26(7): 500–509. https://doi.org/10.2108/zsj.26.500

Wang L, Chen J-Z, Dong Z-M, Chen G-W, Sluys R, Liu D-Z (2021a) Two new species of *Dugesia* (Platyhelminthes, Tricladida, Dugesiidae) from the tropical monsoon forest in Southern China. ZooKeys 1059: 89–116. https://doi.org/10.3897/zookeys.1059.65633

Wang L, Dong Z-M, Chen G-W, Sluys R, Liu D-Z (2021b) Integrative descriptions of two new species of *Dugesia* from Hainan Island, China (Platyhelminthes, Tricladida, Dugesiidae). ZooKeys 1028: 1–28. https://doi.org/10.3897/zookeys.1028.60838

Wang L, Wang Y-X, Dong Z-M, Chen G-W, Sluys R, Liu D-Z (2022) Integrative taxonomy unveils a new species of *Dugesia* (Platyhelminthes, Tricladida, Dugesiidae) from the southern portion of the Taihang Mountains in northern China, with the description of its complete mitogenome and an exploratory analysis of mitochondrial gene order as a taxonomic character. Integrative Zoology 17(6): 1193–1214. https://doi.org/10.1111/1749-4877.12605

Wang L, Zhu S-Q, Ma F-H, Li X-J, Zhao Y-H, Sun X-X, Li N, Sluys R, Liu D-Z, Dong Z-M, Chen G-W (2024) Two new species of freshwater planarian (Platyhelminthes, Tricladida, Dugesiidae, *Dugesia*) from Southern China exhibit unusual karyotypes, with a discussion on reproduction in aneuploid species. Journal of Zoological Systematics and Evolutionary Research 2024: 8299436. https://doi.org/10.1155/2024/8299436

Wang L, Chang Y-F, Sun X-X, Sluys R, Liu D-Z, Dong Z-M, Chen G-W (2025) Two new species of *Dugesia* from Hainan Island and Leizhou Peninsula (Platyhelminthes, Tricladida, Dugesiidae). ZooKeys 1233: 289–313. https://doi.org/10.3897/zookeys.1233.142976

Winsor L, Sluys R (2018) Basic histological techniques for planarians. In: Rink JC (Ed.) Planarian Regeneration: Methods and Protocols. Methods in Molecular Biology, Vol. 1774. Humana Press, Springer Science+Business Media, New York, 285–351. https://doi.org/10.1007/978-1-4939-7802-1_9

Wu F, Wang L, Sluys R, Sun XX, Liu DZ, Dong ZM, Chen GW (2025) An integrative analysis and account of two new species of *Dugesia* (Platyhelminthes, Tricladida, Dugesiidae) from the Hengduan Mountains, southwest China, with reflections on the historical biogeography of Eastern Palearctic/Oriental lineages. Zoosystematics and Evolution 101(4): 1513–1529. https://doi.org/10.3897/zse.101.156742

Wu L, Wang F, Yang J-H, Wang Y-Z, Zhang W-B, Yang L-K, Shi W-B (2020) Meso-Cenozoic uplift of the Taihang Mountains, North China: Evidence from zircon and apatite thermochronology. Geological Magazine 157(7): 1097–1111. https://doi.org/10.1017/S0016756819001377

Zeng Z-Y, Wang J, Sluys R, Guo Z-P, Sun T, Huang X-Z, Li S-F, Wang A-T (2024) Integrative description of a new species of *Dugesia* (Platyhelminthes, Tricladida, Dugesiidae) from Shennongjia, Central China. Zootaxa 5406(4): 535–550. https://doi.org/10.11646/zootaxa.5406.4.3

Zhang D, Gao F, Jakovlić I, Zou H, Zhang J, Li W-X, Wang G-T (2020) PhyloSuite: An integrated and scalable desktop platform for streamlined molecular sequence data management and evolutionary phylogenetics studies. Molecular Ecology Resources 20: 348–355. https://doi.org/10.1111/1755-0998.13096

Zhang J-J, Kapli P, Pavlidis P, Stamatakis A (2013) A general species delimitation method with applications to phylogenetic placements. Bioinformatics (29)22: 2869–2876. https://doi.org/10.1093/bioinformatics/btt499

Zhao B, Yin Z-F, Man X, Wang Q-C (2012) AFLP analysis of genetic variation in wild populations of five rhododendron species in Qinling mountain in China. Biochemical Systematics and Ecology 45: 198–205. https://doi.org/10.1016/j.bse.2012.07.033

Zhong H-W, Zhao X, Yin S-M, Zhao X, Zhao T (2010) Late Cenozoic geomorphology, geochronology and physiography of Yuntaishan in Southern Taihang Mountain, North China. Bulletin of the Geological Society of China 84: 230–239. https://doi.org/10.1111/j.1755-6724.2010.00185.x

Supplementary material 1

Supplementary images

Authors: Yi-Fan Su, Fu-Yu Yu, Fan Wu, Jing-Yi Wang, Ronald Sluys, De-Zeng Liu, Lei Wang, Zi-Mei Dong, Guang-Wen Chen

Data type: docx

Explanation note: **figure S1.** Molecular phylogenetic tree obtained from ML analysis of dataset III. Numbers at nodes indicate support values (bootstrap). New species are indicated in red. Scale bar: substitutions per site. **figure S2.** Summary of ABGD (**A**), ASAP (B), and bPTP (**C, D**) analyses. **A.** ABGD partitions obtained for *COI* sequences. **B.** Summary of ASAP test results obtained for *COI* sequences. **C.** bPTP analysis using the Bayesian approach based on the highest Bayesian-supported solution. **D.** PTP analysis using the Bayesian approach based on the maximum-likelihood solution.

Link: https://doi.org/10.3897/zse.102.181547.suppl1

Supplementary material 2

Primers used for amplification, with their annealing temperatures

Authors: Yi-Fan Su, Fu-Yu Yu, Fan Wu, Jing-Yi Wang, Ronald Sluys, De-Zeng Liu, Lei Wang, Zi-Mei Dong, Guang-Wen Chen

Data type: docx

Link: https://doi.org/10.3897/zse.102.181547.suppl2

Supplementary material 3

Genetic distances for *COI*

Authors: Yi-Fan Su, Fu-Yu Yu, Fan Wu, Jing-Yi Wang, Ronald Sluys, De-Zeng Liu, Lei Wang, Zi-Mei Dong, Guang-Wen Chen

Data type: xls

Explanation note: Highest and lowest distance values between the two new Chinese species and congeners are indicated in blue and red, respectively. Green: distance value between the two new species.

Link: https://doi.org/10.3897/zse.102.181547.suppl3

Supplementary material 4

Genetic distances for *ITS-1*

Authors: Yi-Fan Su, Fu-Yu Yu, Fan Wu, Jing-Yi Wang, Ronald Sluys, De-Zeng Liu, Lei Wang, Zi-Mei Dong, Guang-Wen Chen

Data type: xls

Explanation note: Highest and lowest distance values between the two new Chinese species and congeners are indicated in blue and red, respectively. Green: distance value between the two new species.

Link: https://doi.org/10.3897/zse.102.181547.suppl4